
AP-OOD: Attention Pooling for Out-of-Distribution Detection

Claus Hofmann¹ Christian Huber² Bernhard Lehner²

Daniel Klotz³ Sepp Hochreiter¹ Werner Zellinger⁴

¹ Institute for Machine Learning, JKU LIT SAL IWS Lab,
Johannes Kepler University, Linz, Austria

² Silicon Austria Labs, JKU LIT SAL IWS Lab, Linz, Austria

³ Interdisciplinary Transformation University Austria, Linz, Austria

⁴ ELLIS Unit, LIT AI Lab, Institute for Machine Learning, JKU Linz, Austria
hofmann@ml.jku.at

Abstract

Out-of-distribution (OOD) detection, which maps high-dimensional data into a scalar OOD score, is critical for the reliable deployment of machine learning models. A key challenge in recent research is how to effectively leverage and aggregate token embeddings from language models to obtain the OOD score. In this work, we propose AP-OOD, a novel OOD detection method for natural language that goes beyond simple average-based aggregation by exploiting token-level information. AP-OOD is a semi-supervised approach that flexibly interpolates between unsupervised and supervised settings, enabling the use of limited auxiliary outlier data. Empirically, AP-OOD sets a new state of the art in OOD detection for text: in the unsupervised setting, it reduces the FPR95 (false positive rate at 95% true positives) from 27.77% to 5.91% on XSUM summarization, and from 75.19% to 68.13% on WMT15 En–Fr translation.

1 Introduction

Out-of-distribution (OOD) detection is essential for deploying machine learning models in the real world. In practical settings many models encounter inputs that deviate from the model’s training distribution. For example, a model trained to summarize news articles might also receive a prompt with a cooking recipe. In such situations, models may assign unwarranted confidence to their predictions, leading to erroneous outputs. The purpose of OOD detection is to classify these inputs as OOD such that the system can then, for instance, notify the user that the prediction is uncertain. Our contributions are as follows:

1. We propose AP-OOD, an OOD detection approach for natural language that leverages token-level information to detect OOD sequences.
2. AP-OOD is a semi-supervised approach: It can be applied in unsupervised (i.e., when there exists no knowledge about OOD samples) and supervised settings (i.e., when some OOD data of interest is available to the practitioner), and smoothly interpolates between the two.
3. We show that AP-OOD can improve unsupervised and supervised OOD detection for natural language in summarization and translation.
4. We provide a theoretical motivation for the suitability of AP-OOD for OOD detection

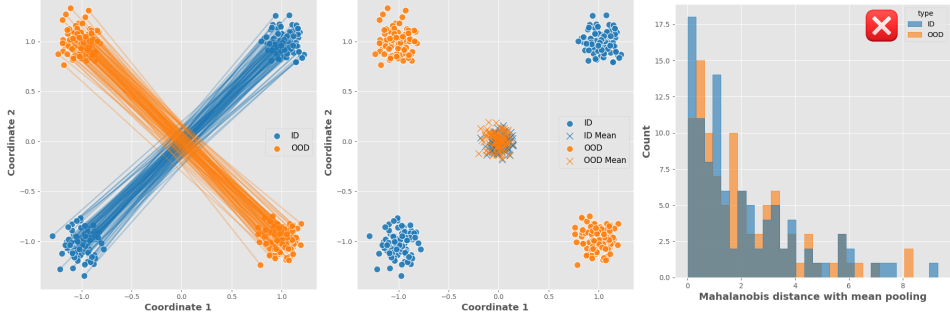


Figure 1: Illustrative example for the failure of mean pooling. **(Left)** ID and OOD sequences $Z_i \in \mathbb{R}^{2 \times 2}$, where each sequence contains a pair of token embeddings with two features each. Token embeddings that belong to the same sequence are connected with lines. **(Center)** The means of the ID and OOD sequences both cluster around the origin. **(Right)** A mean pooling approach cannot discriminate between the ID and OOD sequences.

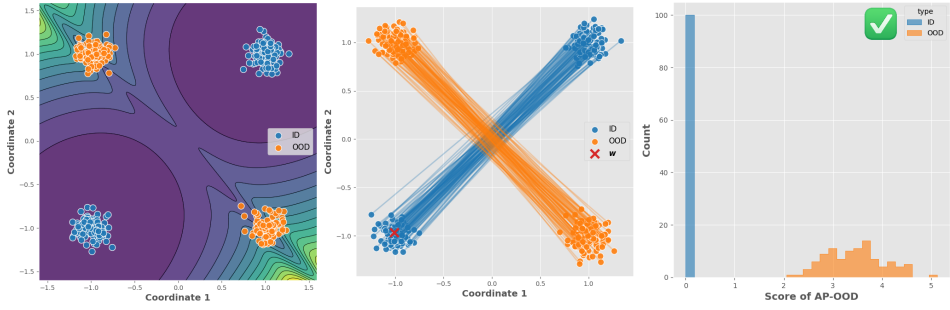


Figure 2: Illustrative example for the mechanism that AP-OOD uses to correctly discriminate between ID and OOD (as opposed to the mean pooling approaches). The setting is the same as in Figure 1. **(Left)** The loss landscape forms two basins at the locations of the ID token embeddings. **(Center)** After training AP-OOD with a single weight vector w , the learned w is located in one of the basins. **(Right)** AP-OOD achieves perfect discrimination between the ID and OOD sequences.

1.1 Background

Consider a language model trained to autoregressively generate target sequences (y_1, y_2, \dots, y_N) given input sequences (x_1, x_2, \dots, x_N). The input sequences are drawn i.i.d.: $x_i \sim p_{\text{ID}}$. We consider input sequences $x \in \mathcal{X}$ ¹ that deviate considerably from the data generation $p_{\text{ID}}(x)$ that defines the “normality” of our data as OOD. Following Ruff et al. (2021), an observed sequence is OOD if it is an element of the set

$$\mathbb{O} := \{x \in \mathcal{X} \mid p_{\text{ID}}(x) < \epsilon\} \text{ where } \epsilon \geq 0, \quad (1)$$

and ϵ is a density threshold. In practice, it is common (e.g., Hendrycks & Gimpel, 2016; Lee et al., 2018; Hofmann et al., 2024) to define a score $s : \mathcal{Z} \rightarrow \mathbb{R}$ that uses an encoder $\phi : \mathcal{X} \rightarrow \mathcal{Z}$ (where \mathcal{Z} denotes an embedding space). Given s and ϕ , OOD detection can be formulated as a binary classification task with the classes in-distribution (ID) and OOD:

$$\hat{B}(x, \gamma) = \begin{cases} \text{ID} & \text{if } s(\phi(x)) \geq \gamma \\ \text{OOD} & \text{if } s(\phi(x)) < \gamma \end{cases}. \quad (2)$$

The outlier score should — in the best case — preserve the density ranking, but it does not have to fulfill all requirements of a probability density (proper normalization or nonnegativity). For evaluation, the threshold γ is typically chosen such that 95% of ID samples from a previously unseen validation set are correctly classified as ID. However, metrics like the area under the receiver operating characteristic (AUROC) can be directly computed on $s(\phi(x))$ without fixing γ , since the AUROC sweeps over all possible thresholds.

¹We use $\mathcal{X} := \bigcup_{S \geq 1} \mathcal{V}^S$ for the set of input sequences, and $\mathcal{V} := \{v_1, \dots, v_V\}$ is the vocabulary.

2 Method

AP-OOD is a semi-supervised method: It can be trained without access to outlier data (unsupervised), and with access to outlier data (supervised), and can smoothly transition between those two scenarios as more outlier data becomes available for training. In the following, we first introduce AP-OOD in an unsupervised scenario (Section 2.1) and generalize it to the supervised scenario (Section 2.2).

2.1 Unsupervised OOD Detection

Background Ren et al. (2023) propose to detect OOD inputs using token embeddings obtained from a transformer encoder–decoder model (Vaswani et al., 2017) trained on the language modeling task. Given an input sequence $\mathbf{x} \in \mathcal{X}$, they obtain a sequence of token embeddings $\mathbf{Z} = (z_1, \dots, z_S) \in \mathbb{R}^{D \times S}$. They compare obtaining embeddings \mathbf{E} from the encoder $\phi_{\text{enc}} : \mathcal{X} \rightarrow \mathcal{Z}$ ² and generating a sequence of embeddings \mathbf{G} using the decoder $\phi_{\text{dec}} : \mathcal{Z} \rightarrow \mathcal{Z}$:

$$\mathbf{E} := \phi_{\text{enc}}(\mathbf{x}) \quad \mathbf{G} := \phi_{\text{dec}}(\mathbf{E}). \quad (3)$$

For clarity, we write \mathbf{Z} for a sequence of token embeddings, whether produced by the encoder or the decoder, and we call \mathbf{Z} the sequence representation of \mathbf{x} . To obtain a single vector $\bar{\mathbf{z}} \in \mathbb{R}^D$, Ren et al. (2023) perform mean pooling:

$$\bar{\mathbf{z}} := \frac{1}{S} \sum_{s=1}^S \mathbf{z}_s. \quad (4)$$

Then, they propose to measure whether $\bar{\mathbf{z}}$ is OOD by first fitting a Gaussian distribution $\mathcal{N}(\boldsymbol{\mu}, \boldsymbol{\Sigma})$, $\boldsymbol{\mu} \in \mathbb{R}^D$, $\boldsymbol{\Sigma} \in \mathbb{R}^{D \times D}$ to the per-sequence mean embeddings computed from the training corpus, and then computing the squared Mahalanobis distance between $\bar{\mathbf{z}}$ and $\boldsymbol{\mu}$:

$$d_{\text{Maha}}^2(\bar{\mathbf{z}}, \boldsymbol{\mu}) := (\bar{\mathbf{z}} - \boldsymbol{\mu})^T \boldsymbol{\Sigma}^{-1} (\bar{\mathbf{z}} - \boldsymbol{\mu}) \quad \text{and} \quad s_{\text{Maha}}(\bar{\mathbf{z}}) := -d_{\text{Maha}}^2(\bar{\mathbf{z}}, \boldsymbol{\mu}). \quad (5)$$

Averaging hides anomalies. The key limitation of the approach described above is the use of the **mean** of the token embeddings \mathbf{Z} : Averaging the entire sequence into the mean $\bar{\mathbf{z}}$ discards the token-level structure that would otherwise be informative for detecting whether a sequence is OOD. Figure 1 shows a toy example of this failure mode: The ID and OOD sequences are indistinguishable using their means, and therefore, the Mahalanobis distance with mean pooling fails to discriminate between them.

Mahalanobis decomposition. To address this limitation, we begin by expressing the Mahalanobis distance as a directional decomposition:

$$d_{\text{Maha}}^2(\bar{\mathbf{z}}, \boldsymbol{\mu}) = \sum_{j=1}^D (\mathbf{w}_j^T \bar{\mathbf{z}} - \mathbf{w}_j^T \boldsymbol{\mu})^2, \quad (6)$$

The weight vectors $\mathbf{w}_j \in \mathbb{R}^D$ form a basis of \mathbb{R}^D and determine $\boldsymbol{\Sigma}^{-1}$ via $\boldsymbol{\Sigma}^{-1} = \sum_{j=1}^D \mathbf{w}_j \mathbf{w}_j^T$. One possibility to map a given $\boldsymbol{\Sigma}^{-1}$ to weight vectors \mathbf{w}_j is to select the directions of the \mathbf{w}_j as the unit-norm eigenvectors of $\boldsymbol{\Sigma}^{-1}$, and to select the squared norms of the \mathbf{w}_j as their corresponding eigenvalues (see Appendix B.2).

Beyond mean pooling. To overcome the limitations of mean pooling, we generalize Equation (6) by using attention pooling (Bahdanau, 2014; Ramsauer et al., 2021):

$$\text{AttPool}_{\beta}(\mathbf{Z}, \mathbf{w}) := \mathbf{Z} \text{softmax}(\beta \mathbf{Z}^T \mathbf{w}) \quad \text{and} \quad \bar{\mathbf{z}} := \text{AttPool}_{\beta}(\mathbf{Z}, \mathbf{w}). \quad (7)$$

where β is the inverse temperature, and \mathbf{w} is a learnable query. AP-OOD also uses attention for the corpus-wide pooling: Given the sequence representations $(\mathbf{Z}_1, \dots, \mathbf{Z}_N)$ from a corpus $(\mathbf{x}_1, \dots, \mathbf{x}_N)$ with $\mathbf{Z}_i := \phi_{\text{enc}}(\mathbf{x}_i)$, we define $\tilde{\mathbf{Z}}$ as the concatenation of all sequence representations: $\tilde{\mathbf{Z}} := (\mathbf{Z}_1 \| \dots \| \mathbf{Z}_N)$. AP-OOD estimates $\boldsymbol{\mu} := \text{AttPool}_{\beta}(\tilde{\mathbf{Z}}, \mathbf{w})$. Given the $\bar{\mathbf{z}}$ and $\boldsymbol{\mu}$ from

²We use $\mathcal{Z} := \bigcup_{S \geq 1} \mathbb{R}^{D \times S}$ for all finite-length sequences of D -dimensional token embeddings.

the attention pooling, AP-OOD estimates $d^2(\mathbf{Z}, \tilde{\mathbf{Z}})$, the squared distance between a sequence representation \mathbf{Z} and the concatenation $\tilde{\mathbf{Z}}$ analogous to Equation (6):

$$d^2(\mathbf{Z}, \tilde{\mathbf{Z}}) := \sum_{j=1}^M \left(\mathbf{w}_j^T \mathbf{Z} \text{softmax}(\beta \mathbf{Z}^T \mathbf{w}_j) - \mathbf{w}_j^T \tilde{\mathbf{Z}} \text{softmax}(\beta \tilde{\mathbf{Z}}^T \mathbf{w}_j) \right)^2 = \sum_{j=1}^M d_j^2(\mathbf{Z}, \tilde{\mathbf{Z}}). \quad (8)$$

We refer to M as the number of heads. In general, M does not need to equal the embedding dimension D . We show in Appendix B.3 that, when $\beta = 0$ and $M = D$, Equation (8) reduces to the Mahalanobis distance (Equations (5) and (6)). In Appendix B.1, we show that $s_{\min}(\mathbf{Z}) = \min_j -d_j^2(\mathbf{Z}, \tilde{\mathbf{Z}}) + \log(\|\mathbf{w}_j\|_2^2)$ is a score function as defined in Equation (2). Our score arises naturally as the upper bound

$$s(\mathbf{Z}) := \sum_{j=1}^M -d_j^2(\mathbf{Z}, \tilde{\mathbf{Z}}) + \log(\|\mathbf{w}_j\|_2^2). \quad (9)$$

In Appendix D.5, we empirically compare the min-based score $s_{\min}(\mathbf{Z})$ to its upper-bound variant $s(\mathbf{Z})$ and find that $s(\mathbf{Z})$ yields stronger OOD discrimination. The choice of this score naturally leads to the loss function of AP-OOD:

$$\mathcal{L}(\mathbf{w}_1, \dots, \mathbf{w}_M) := \frac{1}{N} \sum_{i=1}^N d^2(\mathbf{Z}_i, \tilde{\mathbf{Z}}) - \sum_{j=1}^M \log(\|\mathbf{w}_j\|_2^2). \quad (10)$$

Appendix C.1 gives pseudocode for AP-OOD. Figure 2 shows a toy task that AP-OOD solves, whereas mean-pooling baselines fail. Details of this experiment appear in Appendix D.3.

2.2 Supervised OOD Detection

Background. Supplying an OOD detector with information about the distribution of the OOD examples at training time can improve the ID–OOD decision boundary (Hendrycks et al., 2018). In practice, it is hard to find OOD data for training that is fully indicative of the OOD distribution seen during inference. Outlier exposure (OE; Hendrycks et al., 2018) therefore uses a large and diverse auxiliary outlier set (AUX; e.g., C4 for text data) as a stand-in for the OOD case. However, it is not always possible to crawl such large and diverse AUX data sets. For example, consider a translation task with a less widely spoken source language. In such a case, one might have to resort to a smaller AUX data set. Therefore, it is desirable that an OOD detector scales gracefully with the degree of auxiliary supervision, adapting to the available number of AUX examples (Ruff et al., 2019; Liznerski et al., 2022).

Utilizing AUX data. To adapt AP-OOD to the supervised setting, we follow Ruff et al. (2019) and Liznerski et al. (2022): AP-OOD punishes large squared distances $d^2(\mathbf{Z}, \tilde{\mathbf{Z}})$ for ID samples \mathbf{Z} and encourages large squared distances for AUX samples \mathbf{Z} . Formally, AP-OOD minimizes the binary cross-entropy loss with the classes ID and AUX with $p(y = \text{ID} | \mathbf{Z}) = \exp(-d^2(\mathbf{Z}, \tilde{\mathbf{Z}}))$. Given N ID examples $(\mathbf{Z}_1, \dots, \mathbf{Z}_N)$, and N' AUX examples $(\mathbf{Z}_{N+1}, \dots, \mathbf{Z}_{N+N'})$, AP-OOD minimizes the supervised loss

$$\mathcal{L}_{\text{SUP}} := \frac{1}{N + N'} \sum_{i=1}^N d^2(\mathbf{Z}_i, \tilde{\mathbf{Z}}) - \lambda \frac{1}{N + N'} \sum_{i=N+1}^{N+N'} \log(1 - \exp(-d^2(\mathbf{Z}_i, \tilde{\mathbf{Z}}))), \quad (11)$$

where $\lambda \geq 0$. If $\lambda = 0$, \mathcal{L}_{SUP} equals the unsupervised loss \mathcal{L} without the regularizing term.

3 Experiments

Summarization. We follow Ren et al. (2023) and use a PEGASUS_{LARGE} (Zhang et al., 2020) fine-tuned on the ID data set XSUM (Narayan et al., 2018). We utilize the C4 training split as the AUX data set. We measure the OOD detection performance on the data sets CNN/Daily Mail (CNN/DM; news articles from CNN and Daily Mail; Hermann et al., 2015; See et al., 2017), Newsroom (articles and summaries written by authors and editors from 38 news publications; Grusky et al., 2018), Reddit TIFU (posts and summaries from the online discussion forum Reddit; Kim et al., 2018), and Samsum (summaries of casual dialogues; Gliwa et al., 2019). The ForumSum data set used in the experiments of Ren et al. (2023) has been retracted. Therefore, we do not use it in our experiments.

Table 1: Unsupervised OOD detection performance on text summarization. We compare results from AP-OOD, Mahalanobis (Lee et al., 2018; Ren et al., 2023), KNN (Sun et al., 2022), Deep SVDD (Ruff et al., 2018), model perplexity (Ren et al., 2023), and entropy (Malinin & Gales, 2020) on PEGASUS_{LARGE} trained on XSUM as the ID data set. ↓ indicates “lower is better” and ↑ “higher is better”. All values in %. We estimate standard deviations across five independent data set splits and training runs.

	CNN/DM	Newsroom	Reddit	Samsun	Mean
Input OOD					
Mahalanobis	AUROC ↑	69.00 \pm 0.27	86.37 \pm 0.19	98.64 \pm 0.07	99.77 \pm 0.01
	FPR95 ↓	92.19 \pm 0.08	64.48 \pm 0.71	2.45 \pm 0.34	0.17 \pm 0.02
KNN	AUROC ↑	54.34 \pm 0.15	73.76 \pm 0.09	94.52 \pm 0.03	98.82 \pm 0.01
	FPR95 ↓	99.40 \pm 0.03	88.56 \pm 0.17	51.24 \pm 0.70	3.07 \pm 0.16
Deep SVDD	AUROC ↑	75.86 \pm 1.00	91.20 \pm 0.21	99.73 \pm 0.05	99.57 \pm 0.04
	FPR95 ↓	73.70 \pm 2.35	36.46 \pm 1.12	0.26 \pm 0.09	0.67 \pm 0.17
AP-OOD (Ours)	AUROC ↑	96.13 \pm 0.44	99.10 \pm 0.08	99.91 \pm 0.03	99.80 \pm 0.04
	FPR95 ↓	19.51 \pm 2.24	4.11 \pm 0.28	0.00 \pm 0.01	0.04 \pm 0.03
Output OOD					
Perplexity	AUROC ↑	42.20 \pm 0.14	53.99 \pm 0.31	83.38 \pm 0.15	78.53 \pm 0.31
	FPR95 ↓	77.71 \pm 0.17	79.07 \pm 0.57	45.56 \pm 0.40	46.96 \pm 0.20
Entropy	AUROC ↑	59.59 \pm 0.21	77.20 \pm 0.52	93.47 \pm 0.21	87.17 \pm 0.20
	FPR95 ↓	79.04 \pm 0.75	64.24 \pm 1.21	30.19 \pm 1.34	50.47 \pm 1.64
Mahalanobis	AUROC ↑	63.27 \pm 0.17	88.26 \pm 0.11	97.40 \pm 0.09	97.29 \pm 0.08
	FPR95 ↓	89.84 \pm 0.13	47.83 \pm 0.71	11.13 \pm 0.58	13.57 \pm 0.25
KNN	AUROC ↑	74.37 \pm 0.13	86.96 \pm 0.08	95.85 \pm 0.06	97.33 \pm 0.03
	FPR95 ↓	73.36 \pm 0.20	53.44 \pm 0.58	15.78 \pm 0.27	10.29 \pm 0.22
Deep SVDD	AUROC ↑	68.31 \pm 1.63	94.13 \pm 0.12	97.60 \pm 0.26	95.97 \pm 0.15
	FPR95 ↓	76.76 \pm 1.15	19.22 \pm 0.34	8.90 \pm 1.25	20.17 \pm 1.28
AP-OOD (Ours)	AUROC ↑	93.37 \pm 0.54	92.62 \pm 0.67	98.04 \pm 0.28	98.30 \pm 0.11
	FPR95 ↓	23.12 \pm 1.97	29.91 \pm 2.93	6.34 \pm 1.56	6.83 \pm 0.64

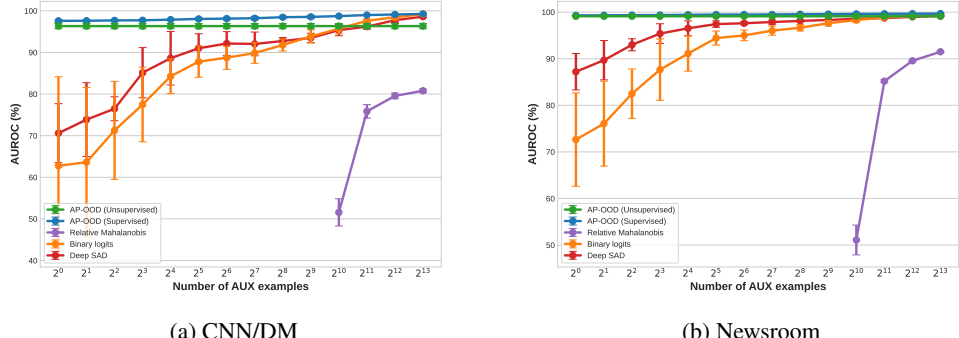
Table 2: Unsupervised OOD detection performance on audio classification. We compare results from AP-OOD, Mahalanobis (Lee et al., 2018; Ren et al., 2023), KNN (Sun et al., 2022), Deep SVDD (Ruff et al., 2018), MSP (Hendrycks & Gimpel, 2016), and EBO (Liu et al., 2020b) trained on MIMII-DG (Dohi et al., 2022) as the ID data set. ↓ indicates “lower is better” and ↑ “higher is better”. All values in %. We estimate standard deviations across five independent training runs.

Mahalanobis	KNN	Deep SVDD	MSP	EBO	AP-OOD (Ours)
AUROC ↑	64.96 \pm 0.002	81.21 \pm 0.000	53.48 \pm 1.930	88.05 \pm 0.000	90.75 \pm 0.000
FPR95 ↓	84.39 \pm 0.011	57.11 \pm 0.000	89.44 \pm 1.689	36.43 \pm 0.000	61.86 \pm 0.000

Training. We extract 100,000 ID sequence representations (E or G) and use all extracted representations for training AP-OOD in all experiments. We also extract AUX sequence representations, and we vary the number of AUX sequences available from 0 (unsupervised) to 10,000 (fully supervised). While training AP-OOD, the transformer model remains frozen. We use the Adam optimizer (Kingma & Ba, 2014) without weight decay, set the learning rate to 0.01, and apply a cosine schedule (Loshchilov & Hutter, 2016). We train for 2,000 steps with a batch size of 512. We select M and T such that the parameter count of AP-OOD matches the parameter count of the Mahalanobis method (i.e., the size of Σ). For more information on hyperparameter selection, we refer to Appendix D.4. During training, we estimate μ using the sequences in a given mini-batch. When training is complete, we do an additional pass over the corpus \tilde{Z} and compute the final μ using attention pooling, which we implement by iterating over mini-batches of \tilde{Z} . We describe this process in Appendix C.2.

Baselines. We compare AP-OOD to five unsupervised OOD detection methods: We apply the embedding-based methods Mahalanobis (Lee et al., 2018; Ren et al., 2023), KNN (Sun et al., 2022), and Deep SVDD (Ruff et al., 2018) to both the input and output sequence representations (E and G , respectively), and we apply Perplexity (Ren et al., 2023) and Entropy (Malinin & Gales, 2020) to the output of the decoder. We also compare AP-OOD to three supervised OOD detection methods: binary logits (Ren et al., 2023), relative Mahalanobis (Ren et al., 2023), and Deep SAD (Ruff et al., 2019). We evaluate the discriminative power of the methods in our comparison using the false positive rate at 95% true positives (FPR95) and AUROC.

Audio data. To demonstrate the effectiveness of AP-OOD on data modalities other than text, we apply the method to the MIMII-DG audio data set (Dohi et al., 2022). The data set comprises



(a) CNN/DM

(b) Newsroom

Figure 3: OOD detection performance on the input token embeddings of PEGASUS_{LARGE} trained on XSUM. We vary the number of AUX samples and compare AP-OOD, binary logits (Ren et al., 2023), Deep SAD (Ruff et al., 2019), and relative Mahalanobis (Ren et al., 2023). AP-OOD attains the highest AUROC independent of AUX sample count.

audio recordings of 15 different machines, ranging from 10 to 12 seconds in length. The dataset contains 990 samples per machine. During preprocessing, the raw audio waveforms are converted into audio spectrograms. We train a transformer to classify a subset of 7 machines. The remaining 8 machines are considered as OOD. The architecture and training method for the network were adopted from Huang et al. (2022). To adjust for the small data set size, we decrease the size of the architecture: We increase the patch size to 32×32 pixels, decrease the embedding dimension to 32, and utilize only three attention blocks with four heads each. Consequently, the encoder of the network produces 128 tokens with $D = 32$ features. We train AP-OOD on the encoder output in the unsupervised setting using $M = 128$ and $T = 8$.

4 Results

Table 1 shows the results on unsupervised OOD detection on the text summarization task. AP-OOD surpasses methods with mean pooling by a large margin for both input and output settings for most OOD data sets. Most notably, the mean FPR95 on CNN/DM improves from 73.70% for the best baseline Deep SVDD to 19.51% for AP-OOD. The table also shows that the embedding-based methods (Mahalanobis, KNN, Deep SVDD, and AP-OOD) perform better than the prediction-based baselines perplexity and entropy. Figure 3 shows the results of AP-OOD in the semi-supervised setting: supplying AUX data to AP-OOD improves the AUROC, and more AUX data results in a larger improvement. AP-OOD attains the highest AUROC independent of AUX sample count. We include the results on additional OOD data sets in the semi-supervised setting and results on fully supervised OOD detection on the summarization task in Appendix D.2, and we present ablations on AP-OOD on text summarization in Appendix D.6.

In the audio task, the network achieves an accuracy of 97.6% on the primary classification task. Table 2 presents the results of the unsupervised OOD detection methods AP-OOD, Mahalanobis (Lee et al., 2018), KNN (Sun et al., 2022), and Deep SVDD (Ruff et al., 2018). The results show that AP-OOD improves the FPR95 metric from 57.11% (KNN) to 22.35%.

5 Conclusion

We introduce AP-OOD: an approach for OOD detection for natural language that can learn in supervised and unsupervised settings. In contrast to previous methods, AP-OOD learns how to pool token-level information without the explicit need for AUX data. Our experiments show that when supplied with AUX data during training, the performance of AP-OOD improves as more AUX data is provided. We compare AP-OOD to five unsupervised and three supervised OOD detection methods. Overall, AP-OOD shows the best results.

Acknowledgements

The ELLIS Unit Linz, the LIT AI Lab, the Institute for Machine Learning, are supported by the Federal State Upper Austria. We thank the projects FWF AIRI FG 9-N (10.55776/FG9), AI4GreenHeatingGrids (FFG- 899943), Stars4Waters (HORIZON-CL6-2021-CLIMATE-01-01), FWF Bilateral Artificial Intelligence (10.55776/COE12). We thank NXAI GmbH, Audi AG, Silicon Austria Labs (SAL), Merck Healthcare KGaA, GLS (Univ. Waterloo), TÜV Holding GmbH, Software Competence Center Hagenberg GmbH, dSPACE GmbH, TRUMPF SE + Co. KG. We acknowledge EuroHPC Joint Undertaking for awarding us access to Karolina at IT4Innovations, Czech Republic and Leonardo at CINECA, Italy.

References

- Lukas Aichberger, Kajetan Schweighofer, Mykyta Ielanskyi, and Sepp Hochreiter. Improving uncertainty estimation through semantically diverse language generation. In *The Thirteenth International Conference on Learning Representations*, 2025.
- Ghadi S Al Hajj, Aliaksandr Hubin, Chakravarthi Kanduri, Milena Pavlovic, Knut Dagestad Rand, Michael Widrich, Anne Schistad Solberg, Victor Greiff, Johan Pensar, Günter Klambauer, et al. Incorporating probabilistic domain knowledge into deep multiple instance learning. In *Forty-first International Conference on Machine Learning*, 2024.
- Stuart Andrews, Ioannis Tschantaridis, and Thomas Hofmann. Support vector machines for multiple-instance learning. *Advances in neural information processing systems*, 15, 2002.
- Andreas Auer, Martin Gauch, Daniel Klotz, and Sepp Hochreiter. Conformal prediction for time series with modern hopfield networks. *Advances in Neural Information Processing Systems*, 36: 56027–56074, 2023.
- Mikko Aulamo and Jörg Tiedemann. The OPUS resource repository: An open package for creating parallel corpora and machine translation services. In Mareike Hartmann and Barbara Plank (eds.), *Proceedings of the 22nd Nordic Conference on Computational Linguistics*, pp. 389–394, Turku, Finland, September–October 2019. Linköping University Electronic Press.
- Dzmitry Bahdanau. Neural machine translation by jointly learning to align and translate. *arXiv preprint arXiv:1409.0473*, 2014.
- Christopher M Bishop. Novelty detection and neural network validation. *IEE Proceedings-Vision, Image and Signal processing*, 141(4):217–222, 1994.
- Ondřej Bojar, Rajen Chatterjee, Christian Federmann, Barry Haddow, Matthias Huck, Chris Hokamp, Philipp Koehn, Varvara Logacheva, Christof Monz, Matteo Negri, Matt Post, Carolina Scarton, Lucia Specia, and Marco Turchi. Findings of the 2015 workshop on statistical machine translation. In Ondřej Bojar, Rajen Chatterjee, Christian Federmann, Barry Haddow, Chris Hokamp, Matthias Huck, Varvara Logacheva, and Pavel Pecina (eds.), *Proceedings of the Tenth Workshop on Statistical Machine Translation*, pp. 1–46, Lisbon, Portugal, September 2015. Association for Computational Linguistics.
- Thomas G Dietterich, Richard H Lathrop, and Tomás Lozano-Pérez. Solving the multiple instance problem with axis-parallel rectangles. *Artificial intelligence*, 89(1-2):31–71, 1997.
- Andrija Djurisic, Nebojsa Bozanic, Arjun Ashok, and Rosanne Liu. Extremely simple activation shaping for out-of-distribution detection. In *The Eleventh International Conference on Learning Representations*, 2023.
- Kota Dohi, Tomoya Nishida, Harsh Purohit, Ryo Tanabe, Takashi Endo, Masaaki Yamamoto, Yuki Nikaido, and Yohei Kawaguchi. MIMII DG: Sound dataset for malfunctioning industrial machine investigation and inspection for domain generalization task. In *Proceedings of the 7th Detection and Classification of Acoustic Scenes and Events 2022 Workshop (DCASE2022)*, Nancy, France, November 2022.
- Xuefeng Du, Zhaoning Wang, Mu Cai, and Yixuan Li. Vos: Learning what you don’t know by virtual outlier synthesis. *arXiv preprint arXiv:2202.01197*, 2022.

- Xuefeng Du, Chaowei Xiao, and Sharon Li. Haloscope: Harnessing unlabeled llm generations for hallucination detection. *Advances in Neural Information Processing Systems*, 37:102948–102972, 2024.
- Sebastian Farquhar, Jannik Kossen, Lorenz Kuhn, and Yarin Gal. Detecting hallucinations in large language models using semantic entropy. *Nature*, 630(8017):625–630, 2024.
- Andreas Fürst, Elisabeth Rumetshofer, Johannes Lehner, Viet T Tran, Fei Tang, Hubert Ramsauer, David Kreil, Michael Kopp, Günter Klambauer, Angela Bitto, et al. CLOOB: Modern Hopfield networks with InfoLOOB outperform clip. *Advances in neural information processing systems*, 35: 20450–20468, 2022.
- Bogdan Gliwa, Iwona Mochol, Maciej Biesek, and Aleksander Wawer. Samsum corpus: A human-annotated dialogue dataset for abstractive summarization. *arXiv preprint arXiv:1911.12237*, 2019.
- Max Grusky, Mor Naaman, and Yoav Artzi. Newsroom: A dataset of 1.3 million summaries with diverse extractive strategies. *arXiv preprint arXiv:1804.11283*, 2018.
- Kaiyu Guo, Zijian Wang, Tan Pan, Brian C Lovell, and Mahsa Baktashmotagh. Improving out-of-distribution detection via dynamic covariance calibration. In *Forty-second International Conference on Machine Learning*, 2025.
- Dan Hendrycks and Kevin Gimpel. A baseline for detecting misclassified and out-of-distribution examples in neural networks. *arXiv preprint arXiv:1610.02136*, 2016.
- Dan Hendrycks, Mantas Mazeika, and Thomas Dietterich. Deep anomaly detection with outlier exposure. *arXiv preprint arXiv:1812.04606*, 2018.
- Dan Hendrycks, Steven Basart, Mantas Mazeika, Andy Zou, Joe Kwon, Mohammadreza Mostajabi, Jacob Steinhardt, and Dawn Song. Scaling out-of-distribution detection for real-world settings. *arXiv preprint arXiv:1911.11132*, 2019a.
- Dan Hendrycks, Mantas Mazeika, and Thomas Dietterich. Deep anomaly detection with outlier exposure. In *International Conference on Learning Representations*, 2019b. URL <https://openreview.net/forum?id=HyxCxhRcY7>.
- Dan Hendrycks, Mantas Mazeika, Saurav Kadavath, and Dawn Song. Using self-supervised learning can improve model robustness and uncertainty. *Advances in neural information processing systems*, 32, 2019c.
- Dan Hendrycks, Andy Zou, Mantas Mazeika, Leonard Tang, Bo Li, Dawn Song, and Jacob Steinhardt. Pixmix: Dreamlike pictures comprehensively improve safety measures. In *Proceedings of the IEEE/CVF Conference on Computer Vision and Pattern Recognition*, pp. 16783–16792, 2022.
- Karl Moritz Hermann, Tomas Kociský, Edward Grefenstette, Lasse Espeholt, Will Kay, Mustafa Suleyman, and Phil Blunsom. Teaching machines to read and comprehend. *Advances in neural information processing systems*, 28, 2015.
- Claus Hofmann, Simon Schmid, Bernhard Lehner, Daniel Klotz, and Sepp Hochreiter. Energy-based hopfield boosting for out-of-distribution detection. *arXiv preprint arXiv:2405.08766*, 2024.
- J. J. Hopfield. Neurons with graded response have collective computational properties like those of two-state neurons. *Proceedings of the National Academy of Sciences*, 81(10):3088–3092, 1984. doi: 10.1073/pnas.81.10.3088.
- Po-Yao Huang, Hu Xu, Juncheng Li, Alexei Baevski, Michael Auli, Wojciech Galuba, Florian Metze, and Christoph Feichtenhofer. Masked autoencoders that listen. In *NeurIPS*, 2022.
- Maximilian Ilse, Jakub Tomczak, and Max Welling. Attention-based deep multiple instance learning. In *International conference on machine learning*, pp. 2127–2136. PMLR, 2018.
- Wenyu Jiang, Hao Cheng, MingCai Chen, Chongjun Wang, and Hongxin Wei. DOS: Diverse outlier sampling for out-of-distribution detection. In *The Twelfth International Conference on Learning Representations*, 2024. URL <https://openreview.net/forum?id=iriEqxFB4y>.

Byeongchang Kim, Hyunwoo Kim, and Gunhee Kim. Abstractive summarization of reddit posts with multi-level memory networks. *arXiv preprint arXiv:1811.00783*, 2018.

Diederik P Kingma and Jimmy Ba. Adam: A method for stochastic optimization. *arXiv preprint arXiv:1412.6980*, 2014.

Kimin Lee, Kibok Lee, Honglak Lee, and Jinwoo Shin. A simple unified framework for detecting out-of-distribution samples and adversarial attacks. *Advances in neural information processing systems*, 31, 2018.

Weitang Liu, Xiaoyun Wang, John Owens, and Yixuan Li. Energy-based out-of-distribution detection. In H. Larochelle, M. Ranzato, R. Hadsell, M.F. Balcan, and H. Lin (eds.), *Advances in Neural Information Processing Systems*, volume 33, pp. 21464–21475. Curran Associates, Inc., 2020a. URL <https://proceedings.neurips.cc/paper/2020/file/f5496252609c43eb8a3d147ab9b9c006-Paper.pdf>.

Weitang Liu, Xiaoyun Wang, John Owens, and Yixuan Li. Energy-based out-of-distribution detection. *Advances in neural information processing systems*, 33:21464–21475, 2020b.

Xixi Liu, Yaroslava Lochman, and Christopher Zach. Gen: Pushing the limits of softmax-based out-of-distribution detection. In *Proceedings of the IEEE/CVF Conference on Computer Vision and Pattern Recognition*, pp. 23946–23955, 2023.

Philipp Liznerski, Lukas Ruff, Robert A Vandermeulen, Billy Joe Franks, Klaus-Robert Müller, and Marius Kloft. Exposing outlier exposure: What can be learned from few, one, and zero outlier images. *arXiv preprint arXiv:2205.11474*, 2022.

Ilya Loshchilov and Frank Hutter. Sgdr: Stochastic gradient descent with warm restarts. *arXiv preprint arXiv:1608.03983*, 2016.

Ilya Loshchilov and Frank Hutter. Decoupled weight decay regularization. *arXiv preprint arXiv:1711.05101*, 2017.

Haodong Lu, Dong Gong, Shuo Wang, Jason Xue, Lina Yao, and Kristen Moore. Learning with mixture of prototypes for out-of-distribution detection. In *The Twelfth International Conference on Learning Representations*, 2024. URL <https://openreview.net/forum?id=uNkKaD3MCs>.

Andrey Malinin and Mark Gales. Uncertainty estimation in autoregressive structured prediction. *arXiv preprint arXiv:2002.07650*, 2020.

Andrey Malinin, Neil Band, German Chesnokov, Yarin Gal, Mark JF Gales, Alexey Noskov, Andrey Ploskonosov, Liudmila Prokhorenkova, Ivan Provilkov, Vatsal Raina, et al. Shifts: A dataset of real distributional shift across multiple large-scale tasks. *arXiv preprint arXiv:2107.07455*, 2021.

Oded Maron and Tomás Lozano-Pérez. A framework for multiple-instance learning. *Advances in neural information processing systems*, 10, 1997.

Yifei Ming, Ying Fan, and Yixuan Li. POEM: Out-of-distribution detection with posterior sampling. In Kamalika Chaudhuri, Stefanie Jegelka, Le Song, Csaba Szepesvari, Gang Niu, and Sivan Sabato (eds.), *Proceedings of the 39th International Conference on Machine Learning*, volume 162 of *Proceedings of Machine Learning Research*, pp. 15650–15665. PMLR, 17–23 Jul 2022. URL <https://proceedings.mlr.press/v162/ming22a.html>.

Yifei Ming, Yiyu Sun, Ousmane Dia, and Yixuan Li. How to exploit hyperspherical embeddings for out-of-distribution detection? In *The Eleventh International Conference on Learning Representations*, 2023.

Maximilian Müller and Matthias Hein. Mahalanobis++: Improving ood detection via feature normalization. In *Forty-second International Conference on Machine Learning*, 2025.

Shashi Narayan, Shay B Cohen, and Mirella Lapata. Don’t give me the details, just the summary! topic-aware convolutional neural networks for extreme summarization. *arXiv preprint arXiv:1808.08745*, 2018.

Fabian Paischer, Thomas Adler, Vihang Patil, Angela Bitto-Nemling, Markus Holzleitner, Sebastian Lehner, Hamid Eghbal-Zadeh, and Sepp Hochreiter. History compression via language models in reinforcement learning. In *International Conference on Machine Learning*, pp. 17156–17185. PMLR, 2022.

Seongheon Park, Xuefeng Du, Min-Hsuan Yeh, Haobo Wang, and Yixuan Li. Steer llm latents for hallucination detection. *arXiv preprint arXiv:2503.01917*, 2025.

H. Ramsauer, B. Schäfl, J. Lehner, P. Seidl, M. Widrich, L. Gruber, M. Holzleitner, M. Pavlović, G. K. Sandve, V. Greiff, D. Kreil, M. Kopp, G. Klambauer, J. Brandstetter, and S. Hochreiter. Hopfield networks is all you need. In *9th International Conference on Learning Representations (ICLR)*, 2021. URL <https://openreview.net/forum?id=tL89RnzIicD>.

Jie Ren, Jiaming Luo, Yao Zhao, Kundan Krishna, Mohammad Saleh, Balaji Lakshminarayanan, and Peter J Liu. Out-of-distribution detection and selective generation for conditional language models. In *The Eleventh International Conference on Learning Representations*, 2023. URL <https://openreview.net/forum?id=kJUS5nD0vPB>.

Karsten Roth, Latha Pemula, Joaquin Zepeda, Bernhard Schölkopf, Thomas Brox, and Peter Gehler. Towards total recall in industrial anomaly detection. In *Proceedings of the IEEE/CVF Conference on Computer Vision and Pattern Recognition*, pp. 14318–14328, 2022.

Lukas Ruff, Robert Vandermeulen, Nico Goernitz, Lucas Deecke, Shoaib Ahmed Siddiqui, Alexander Binder, Emmanuel Müller, and Marius Kloft. Deep one-class classification. In *International conference on machine learning*, pp. 4393–4402. PMLR, 2018.

Lukas Ruff, Robert A Vandermeulen, Nico Görnitz, Alexander Binder, Emmanuel Müller, Klaus-Robert Müller, and Marius Kloft. Deep semi-supervised anomaly detection. *arXiv preprint arXiv:1906.02694*, 2019.

Lukas Ruff, Jacob R Kauffmann, Robert A Vandermeulen, Grégoire Montavon, Wojciech Samek, Marius Kloft, Thomas G Dietterich, and Klaus-Robert Müller. A unifying review of deep and shallow anomaly detection. *Proceedings of the IEEE*, 109(5):756–795, 2021.

Ana Sanchez-Fernandez, Elisabeth Rumetschofer, Sepp Hochreiter, and Guenter Klambauer. CLOOME: a new search engine unlocks bioimaging databases for queries with chemical structures. *bioRxiv*, 2022.

Bernhard Schäfl, Lukas Gruber, Angela Bitto-Nemling, and Sepp Hochreiter. Hopular: Modern Hopfield networks for tabular data. *arXiv preprint arXiv:2206.00664*, 2022.

Johannes Schimunek, Philipp Seidl, Lukas Friedrich, Daniel Kuhn, Friedrich Rippmann, Sepp Hochreiter, and Günter Klambauer. Context-enriched molecule representations improve few-shot drug discovery. In *The Eleventh International Conference on Learning Representations*, 2023.

Bernhard Schölkopf, Robert C Williamson, Alex Smola, John Shawe-Taylor, and John Platt. Support vector method for novelty detection. *Advances in neural information processing systems*, 12, 1999.

Bernhard Schölkopf, John C Platt, John Shawe-Taylor, Alex J Smola, and Robert C Williamson. Estimating the support of a high-dimensional distribution. *Neural computation*, 13(7):1443–1471, 2001.

Abigail See, Peter J Liu, and Christopher D Manning. Get to the point: Summarization with pointer-generator networks. *arXiv preprint arXiv:1704.04368*, 2017.

Vikash Sehwag, Mung Chiang, and Prateek Mittal. Ssd: A unified framework for self-supervised outlier detection. *arXiv preprint arXiv:2103.12051*, 2021.

Zhuchen Shao, Hao Bian, Yang Chen, Yifeng Wang, Jian Zhang, Xiangyang Ji, et al. Transmil: Transformer based correlated multiple instance learning for whole slide image classification. *Advances in neural information processing systems*, 34:2136–2147, 2021.

Yiyou Sun, Chuan Guo, and Yixuan Li. React: Out-of-distribution detection with rectified activations. *Advances in Neural Information Processing Systems*, 34:144–157, 2021.

- Yiyou Sun, Yifei Ming, Xiaojin Zhu, and Yixuan Li. Out-of-distribution detection with deep nearest neighbors. In *International Conference on Machine Learning*, pp. 20827–20840. PMLR, 2022.
- Jihoon Tack, Sangwoo Mo, Jongheon Jeong, and Jinwoo Shin. Csi: Novelty detection via contrastive learning on distributionally shifted instances. *Advances in neural information processing systems*, 33:11839–11852, 2020.
- Leitian Tao, Xuefeng Du, Xiaojin Zhu, and Yixuan Li. Non-parametric outlier synthesis. *arXiv preprint arXiv:2303.02966*, 2023.
- David MJ Tax and Robert PW Duin. Support vector data description. *Machine learning*, 54(1):45–66, 2004.
- Jörg Tiedemann. Parallel data, tools and interfaces in opus. In *Lrec*, volume 2012, pp. 2214–2218. Citeseer, 2012.
- Ashish Vaswani, Noam Shazeer, Niki Parmar, Jakob Uszkoreit, Llion Jones, Aidan N Gomez, Łukasz Kaiser, and Illia Polosukhin. Attention is all you need. *Advances in neural information processing systems*, 30, 2017.
- Haoqi Wang, Zhizhong Li, Litong Feng, and Wayne Zhang. Vim: Out-of-distribution with virtual-logit matching. In *Proceedings of the IEEE/CVF conference on computer vision and pattern recognition*, pp. 4921–4930, 2022.
- Qizhou Wang, Zhen Fang, Yonggang Zhang, Feng Liu, Yixuan Li, and Bo Han. Learning to augment distributions for out-of-distribution detection. In *NeurIPS*, 2023. URL <https://openreview.net/forum?id=OtU6VvXJue>.
- Yiming Wang, Pei Zhang, Baosong Yang, Derek Wong, Zhuosheng Zhang, and Rui Wang. Embedding trajectory for out-of-distribution detection in mathematical reasoning. *Advances in Neural Information Processing Systems*, 37:42965–42999, 2024.
- Hongxin Wei, RENCHUNZI Xie, Hao Cheng, Lei Feng, Bo An, and Yixuan Li. Mitigating neural network overconfidence with logit normalization. In *International conference on machine learning*, pp. 23631–23644. PMLR, 2022.
- M. Widrich, B. Schäfl, M. Pavlović, H. Ramsauer, L. Gruber, M. Holzleitner, J. Brandstetter, G. K. Sandve, V. Greiff, S. Hochreiter, and G. Klambauer. Modern Hopfield networks and attention for immune repertoire classification. *ArXiv*, 2007.13505, 2020a.
- Michael Widrich, Bernhard Schäfl, Milena Pavlović, Hubert Ramsauer, Lukas Gruber, Markus Holzleitner, Johannes Brandstetter, Geir Kjetil Sandve, Victor Greiff, Sepp Hochreiter, et al. Modern hopfield networks and attention for immune repertoire classification. *Advances in neural information processing systems*, 33:18832–18845, 2020b.
- Tim Z Xiao, Aidan N Gomez, and Yarin Gal. Wat zei je? detecting out-of-distribution translations with variational transformers. *arXiv preprint arXiv:2006.08344*, 2020.
- Kai Xu, Rongyu Chen, Gianni Franchi, and Angela Yao. Scaling for training time and post-hoc out-of-distribution detection enhancement. In *The Twelfth International Conference on Learning Representations*, 2024.
- Jingkang Yang, Pengyun Wang, Dejian Zou, Zitang Zhou, Kunyuan Ding, Wenxuan Peng, Haoqi Wang, Guangyao Chen, Bo Li, Yiyou Sun, et al. Openood: Benchmarking generalized out-of-distribution detection. *Advances in Neural Information Processing Systems*, 35:32598–32611, 2022.
- Jingqing Zhang, Yao Zhao, Mohammad Saleh, and Peter Liu. Pegasus: Pre-training with extracted gap-sentences for abstractive summarization. In *International conference on machine learning*, pp. 11328–11339. PMLR, 2020.
- Jingyang Zhang, Nathan Inkawich, Randolph Linderman, Yiran Chen, and Hai Li. Mixture outlier exposure: Towards out-of-distribution detection in fine-grained environments. In *Proceedings of the IEEE/CVF Winter Conference on Applications of Computer Vision (WACV)*, pp. 5531–5540, January 2023a.

Jinsong Zhang, Qiang Fu, Xu Chen, Lun Du, Zelin Li, Gang Wang, Shi Han, Dongmei Zhang, et al. Out-of-distribution detection based on in-distribution data patterns memorization with modern Hopfield energy. In *The Eleventh International Conference on Learning Representations*, 2023b.

Jianing Zhu, Yu Geng, Jiangchao Yao, Tongliang Liu, Gang Niu, Masashi Sugiyama, and Bo Han. Diversified outlier exposure for out-of-distribution detection via informative extrapolation. *Advances in Neural Information Processing Systems*, 36, 2023.

Appendix

Table of Contents

A Related Work	14
B Theoretical Notes	16
B.1 OOD Score Investigation	16
B.2 Mahalanobis Decomposition	16
B.3 AP-OOD Reduces to Mahalanobis Distance with Mean Pooling for $\beta = 0$	17
C Additional Algorithmic Details	18
C.1 AP-OOD Algorithmic Overview	18
C.2 Attention Pooling over the Corpus	18
C.3 Extension: Multiple Queries per Head	18
D Experiments	20
D.1 Translation	20
D.2 Additional Experiments on Text Summarization	21
D.3 Toy Experiment	22
D.4 Hyperparameter selection.	22
D.5 OOD score comparison	23
D.6 Ablations	24

A Related Work

OOD detection. Some authors (e.g., Bishop, 1994; Roth et al., 2022; Yang et al., 2022) distinguish between anomalies, outliers, and novelties. These distinctions reflect different goals within applications (Ruff et al., 2021). For example, when an anomaly is found, it will usually be removed from the training pipeline. However, when a novelty is found, it should be studied. We focus on detecting samples that are not part of the training distribution and consider sample categorization as a downstream task. OOD detection methods can be categorized into three groups: Post-hoc, training-time, and OE methods. A common and straightforward approach for OOD detection is the post-hoc approach, where one employs statistics obtained from a classifier. Perhaps the most well-known approach is the maximum softmax probability (MSP; Hendrycks & Gimpel, 2016). A wide range of post-hoc OOD detection approaches have been proposed to address the shortcomings of MSP (e.g., Lee et al., 2018; Hendrycks et al., 2019a; Liu et al., 2020a; Sun et al., 2021, 2022; Wang et al., 2022; Zhang et al., 2023b; Djurisic et al., 2023; Liu et al., 2023; Xu et al., 2024; Guo et al., 2025). A commonly used post-hoc method is the Mahalanobis distance (e.g., Lee et al., 2018; Sehwag et al., 2021; Ren et al., 2023). Recently, Müller & Hein (2025) proposed feature normalization to improve Mahalanobis-based OOD detection, and Guo et al. (2025) show that the Mahalanobis distance benefits from dynamically adjusting the prior geometry in response to new data. In contrast to post-hoc methods, training-time methods modify the training process of the encoder (e.g., Hendrycks et al., 2019c; Tack et al., 2020; Sehwag et al., 2021; Du et al., 2022; Hendrycks et al., 2022; Wei et al., 2022; Ming et al., 2023; Tao et al., 2023; Lu et al., 2024). Finally, the group of OE methods incorporates AUX data in the training process (e.g., Hendrycks et al., 2019b; Liu et al., 2020a; Ming et al., 2022; Zhang et al., 2023a; Wang et al., 2023; Zhu et al., 2023; Jiang et al., 2024; Hofmann et al., 2024).

OOD detection and natural language. Most of the aforementioned OOD detection approaches target vision tasks, and many of them require a classification model as the encoder ϕ . Applying these vision-based OOD methods to text is not straightforward due to the sequence-dependent nature of natural language (e.g., in autoregressive language generation). OOD detection specifically tailored for natural language is still underexplored. Ren et al. (2023) propose the log-model perplexity of a generated sequence \mathbf{y} as a simple baseline for OOD detection on autoregressive language modeling tasks: $-\frac{1}{L} \sum_{l=1}^L \log p_\theta(y_l | \mathbf{y}_{<l}, \mathbf{x})$. However, they show experimentally that model perplexity is inherently limited. Because of these shortcomings, Ren et al. (2023) propose embedding-based OOD detection methods for text data. Relatively few other works have explored OOD detection for generative language modeling. Notable applications include translation (e.g., Xiao et al., 2020; Malinin et al., 2021; Ren et al., 2023), summarization (Ren et al., 2023), and mathematical reasoning (Wang et al., 2024). A related field is hallucination detection (e.g., Malinin & Gales, 2020; Farquhar et al., 2024; Du et al., 2024; Aichberger et al., 2025; Park et al., 2025). Unlike OOD detection (which flags inputs outside the training distribution), the goal of hallucination detection is to identify prompts a generative language model is unlikely to answer truthfully.

Continuous modern Hopfield networks. Modern Hopfield networks (MHNs) are energy-based associative memory networks. They advance conventional Hopfield networks (Hopfield, 1984) by introducing continuous queries and states and a new energy function. MHNs have exponential storage capacity, while retrieval is possible with a one-step update (Ramsauer et al., 2021). The update rule of MHNs coincides with attention as it is used in the Transformer (Vaswani et al., 2017). Examples for successful applications of MHNs are Widrich et al. (2020a); Fürst et al. (2022); Sanchez-Fernandez et al. (2022); Paischer et al. (2022); Schäfl et al. (2022); Schimunek et al. (2023); Auer et al. (2023) and Hofmann et al. (2024).

Multiple instance learning (MIL). MIL (Dietterich et al., 1997; Maron & Lozano-Pérez, 1997; Andrews et al., 2002; Ilse et al., 2018) considers a classifier that maps a bag $Z = (z_1, \dots, z_S)$ of instances z_s to a bag-level label $Y \in \{0, 1\}$. MIL also assumes that individual labels $y_s \in \{0, 1\}$ exist for the instances, which remain unknown during training. By assumption, the bag-level label is positive once one of the instance-level labels is positive (and negative if all are instance-level labels negative), i.e., $Y := \max_s y_s$. Recent MIL methods use attention pooling (Ilse et al., 2018; Shao et al., 2021; Al Hajj et al., 2024) and modern Hopfield networks (Widrich et al., 2020b) to pool the features of the instances.

One-class classification (OCC). OCC (Schölkopf et al., 1999) is the problem of learning a decision boundary separating the ID and OOD regions while having access to examples from the ID data set only. One-Class SVM (Schölkopf et al., 2001) learns a maximum margin hyperplane in the feature space that separates the ID data from the origin. Support Vector Data Description (SVDD; Tax & Duin, 2004) learns a hypersphere which encapsulates the ID data. Most closely related to AP-OOD is Deep SVDD (Ruff et al., 2018). Deep SVDD learns an encoder $\psi(\cdot, \mathcal{W}) : \mathbb{R}^D \rightarrow \mathbb{R}^M$ by minimizing the volume of a data-enclosing hypersphere in the output space. Ruff et al. (2019) propose Deep SAD, an extension of Deep SVDD that makes use of AUX data during training. However, Liznerski et al. (2022) show that the effectiveness of this extension degrades with increasing dimensionality.

B Theoretical Notes

B.1 OOD Score Investigation

In the following, we show that

$$\min_{j \in \{1, \dots, M\}} -d_j^2(\phi_{\text{enc}}(\mathbf{x}), \tilde{\mathbf{Z}}) + \log(\|\mathbf{w}_j\|_2^2) < 2 \log(\epsilon) + \log(2\pi) \implies \mathbf{x} \in \mathbb{O}$$

whenever $z_j := \frac{\mathbf{w}_j^T}{\|\mathbf{w}_j\|_2} \tilde{\mathbf{z}}$ is normally distributed with probability density function

$$\dot{p}_j(z_j) := \frac{\|\mathbf{w}_j\|_2}{\sqrt{2\pi}} \exp\left(-\frac{1}{2}(\|\mathbf{w}_j\|_2 z_j - \mathbf{w}_j^T \boldsymbol{\mu}_j)^2\right), \quad (12)$$

weight vectors $\mathbf{w}_j \in \mathbb{R}^D$, encoder $\phi_{\text{enc}} : \mathcal{X} \rightarrow \mathcal{Z}$, $\mathcal{Z} = \bigcup_{S \geq 1} \mathbb{R}^{D \times S}$, $\mathbf{Z} \in \mathcal{Z}$, $\tilde{\mathbf{Z}} \in \mathcal{Z}$, $\tilde{\mathbf{z}}_j = \mathbf{Z}\mathbf{p}_j$, $\boldsymbol{\mu}_j = \tilde{\mathbf{Z}}\tilde{\mathbf{p}}_j$, $\mathbf{p}_j \in \Delta^S$ and $\tilde{\mathbf{p}}_j \in \Delta^{S'}$ with

$$\Delta^S := \{(p_1, \dots, p_S) \in [0, 1]^S \mid \sum_{i=1}^S p_i = 1\}.$$

Proof. Note that the ϕ_{enc} -pushforward density $p_{\phi_{\text{enc}}}$ of p_{ID} satisfies

$$p_{\phi_{\text{enc}}}(\mathbf{Z}) := \int_{\mathcal{X}} p_{\text{ID}}(\mathbf{x}) \delta(\phi_{\text{enc}}(\mathbf{x}) = \mathbf{Z}) d\mathbf{x} \geq p_{\text{ID}}(\mathbf{x}).$$

Analogously, we get $\bar{p}_j(\tilde{\mathbf{z}}_j) \geq p_{\phi_{\text{enc}}}(\mathbf{Z})$ for $\tilde{\mathbf{z}}_j := \mathbf{Z}\mathbf{p}_j$ and $\dot{p}_j(z_j) \geq \bar{p}_j(\tilde{\mathbf{z}}_j)$ for $z_j := \frac{\mathbf{w}_j^T}{\|\mathbf{w}_j\|_2} \tilde{\mathbf{z}}_j$.

That is, for any $j \in \{1, \dots, M\}$, we have that $p_{\text{ID}}(\mathbf{x}) \leq p_{\phi_{\text{enc}}}(\mathbf{Z}) \leq \bar{p}_j(\tilde{\mathbf{z}}_j) \leq \dot{p}_j(z_j)$. As a consequence, for all $j \in \{1, \dots, M\}$ it holds that $\dot{p}_j(z_j) < \epsilon \implies p_{\text{ID}}(\mathbf{x}) < \epsilon$. Moreover, the following equivalence holds:

$$\begin{aligned} \dot{p}_j(z_j) &< \epsilon &\iff \\ \frac{\|\mathbf{w}_j\|_2}{\sqrt{2\pi}} \exp\left(-\frac{1}{2}(\|\mathbf{w}_j\|_2 z_j - \mathbf{w}_j^T \boldsymbol{\mu}_j)^2\right) &< \epsilon &\iff \\ \frac{\|\mathbf{w}_j\|_2}{\sqrt{2\pi}} \exp\left(-\frac{1}{2}(\mathbf{w}_j^T \tilde{\mathbf{z}}_j - \mathbf{w}_j^T \boldsymbol{\mu}_j)^2\right) &< \epsilon &\iff \\ -(\mathbf{w}_j^T \tilde{\mathbf{z}}_j - \mathbf{w}_j^T \boldsymbol{\mu}_j)^2 + \log(\|\mathbf{w}_j\|_2^2) &< 2 \log(\epsilon) + \log(2\pi) \end{aligned} \quad (13)$$

As a consequence, we have that $\mathbf{x} \in \mathbb{O}$, if Equation (13) is satisfied for any $j \in \{1, \dots, M\}$. \square

B.2 Mahalanobis Decomposition

We assume the D weight vectors \mathbf{w}_j are linearly independent. First, we start from the decomposed term and show that the Mahalanobis distance is equivalent.

$$d_{\text{Maha}}^2(\bar{\mathbf{z}}, \boldsymbol{\mu}) = \sum_{j=1}^D (\mathbf{w}_j^T \bar{\mathbf{z}} - \mathbf{w}_j^T \boldsymbol{\mu})^2 \quad (14)$$

$$= (\bar{\mathbf{z}} - \boldsymbol{\mu})^T \left(\sum_{i=1}^D \mathbf{w}_i \mathbf{w}_i^T \right) (\bar{\mathbf{z}} - \boldsymbol{\mu}) \quad (15)$$

$$= (\bar{\mathbf{z}} - \boldsymbol{\mu})^T \boldsymbol{\Sigma}^{-1} (\bar{\mathbf{z}} - \boldsymbol{\mu}). \quad (16)$$

Because the weight vectors are linearly independent, $\boldsymbol{\Sigma}^{-1}$ has full rank. Next, we go in the opposite direction and show that the eigenvectors $\mathbf{V} = (\mathbf{v}_1, \dots, \mathbf{v}_D)$ and eigenvalues $\mathbf{D} = \text{diag}(\lambda_1, \dots, \lambda_D)$ of $\boldsymbol{\Sigma}$ can be used to select the corresponding \mathbf{w}_j .

$$d_{\text{Maha}}^2(\bar{\mathbf{z}}, \boldsymbol{\mu}) = (\bar{\mathbf{z}} - \boldsymbol{\mu})^T \boldsymbol{\Sigma}^{-1} (\bar{\mathbf{z}} - \boldsymbol{\mu}) \quad (17)$$

$$= (\bar{\mathbf{z}} - \boldsymbol{\mu})^T \mathbf{V}^T \mathbf{D}^{-1} \mathbf{V} (\bar{\mathbf{z}} - \boldsymbol{\mu}) \quad (18)$$

$$= \left(\sqrt{\mathbf{D}^{-1}} \mathbf{V} \bar{\mathbf{z}} - \sqrt{\mathbf{D}^{-1}} \mathbf{V} \boldsymbol{\mu} \right)^T \left(\sqrt{\mathbf{D}^{-1}} \mathbf{V} \bar{\mathbf{z}} - \sqrt{\mathbf{D}^{-1}} \mathbf{V} \boldsymbol{\mu} \right) \quad (19)$$

$$= \sum_{j=1}^D (\mathbf{w}_j^T \bar{\mathbf{z}} - \mathbf{w}_j^T \boldsymbol{\mu})^2, \quad (20)$$

where $\mathbf{w}_j = \sqrt{\lambda_j^{-1}} \mathbf{v}_j$, $\boldsymbol{\Sigma} = \mathbf{V}^T \mathbf{D} \mathbf{V}$, and $\boldsymbol{\Sigma}^{-1} = \mathbf{V}^T \mathbf{D}^{-1} \mathbf{V}$.

B.3 AP-OOD Reduces to Mahalanobis Distance with Mean Pooling for $\beta = 0$

In this section, we show that as $\beta = 0$ and $M = D$, $d^2(\mathbf{Z}, \tilde{\mathbf{Z}})$ reduces to the Mahalanobis distance with mean pooling as used by [Ren et al. \(2023\)](#). To arrive at the result, we assume uniform sequence lengths.

$$\text{softmax}(0 \cdot \mathbf{Z}^T \mathbf{w})_s = \frac{\exp(0 \cdot \mathbf{z}_s^T \mathbf{w})}{\sum_{s'=1}^S \exp(0 \cdot \mathbf{z}_{s'}^T \mathbf{w})} = \frac{1}{S}, \quad (21)$$

$$\bar{\mathbf{z}} = \text{AttPool}_0(\mathbf{Z}, \mathbf{w}) = \mathbf{Z} \text{softmax}(0 \cdot \mathbf{Z}^T \mathbf{w}) = \frac{1}{S} \sum_{s=1}^S \mathbf{z}_s, \quad (22)$$

$$\boldsymbol{\mu} = \text{AttPool}_0(\tilde{\mathbf{Z}}, \mathbf{w}) = \tilde{\mathbf{Z}} \text{softmax}(0 \cdot \tilde{\mathbf{Z}}^T \mathbf{w}) = \frac{1}{SN} \sum_{i=1}^N \sum_{s=1}^S \mathbf{z}_{is} = \frac{1}{N} \sum_{i=1}^N \bar{\mathbf{z}}_i, \quad (23)$$

where we use the concatenated sequence $\tilde{\mathbf{Z}} = (\mathbf{Z}_1 \| \dots \| \mathbf{Z}_N)$, and the sequence representations $\mathbf{Z}_i = \phi(\mathbf{x}_i) = (\mathbf{z}_{i1}, \dots, \mathbf{z}_{iS}) \in \mathbb{R}^{D \times S}$. The squared distance of AP-OOD reduces to

$$d^2(\mathbf{Z}, \tilde{\mathbf{Z}}) = \sum_{j=1}^M \left(\mathbf{w}_j^T \mathbf{Z} \text{softmax}(\beta \mathbf{Z}^T \mathbf{w}_j) - \mathbf{w}_j^T \tilde{\mathbf{Z}} \text{softmax}(\beta \tilde{\mathbf{Z}}^T \mathbf{w}_j) \right)^2 \quad (24)$$

$$= \sum_{j=1}^D (\mathbf{w}_j^T \bar{\mathbf{z}} - \mathbf{w}_j^T \boldsymbol{\mu})^2 = d_{\text{Maha}}^2(\bar{\mathbf{z}}, \boldsymbol{\mu}). \quad (25)$$

To show the relation with non-uniform sequence lengths, we modify the attention pooling as follows:

$$\text{AttPool}_\beta(\mathbf{Z}, \mathbf{w}) := \mathbf{Z} \text{softmax}(\beta \mathbf{Z}^T \mathbf{w} + \log(\mathbf{s})) \quad (26)$$

where \mathbf{s} contains the sequence lengths S of the sequences (replicated for the individual tokens). The corresponding vector $\tilde{\mathbf{s}}$ for $\tilde{\mathbf{Z}}$ consists of the sequence lengths S_i replicated for the individual tokens. The resulting $\bar{\mathbf{z}}$ and $\boldsymbol{\mu}$ are:

$$\text{softmax}(0 \cdot \mathbf{Z}^T \mathbf{w} + \log(\mathbf{s}))_s = \frac{\exp(0 \cdot \mathbf{z}_s^T \mathbf{w} + \log(S))}{\sum_{s'=1}^S \exp(0 \cdot \mathbf{z}_{s'}^T \mathbf{w} + \log(S))} = \frac{1}{S}, \quad (27)$$

$$\bar{\mathbf{z}} = \text{AttPool}_0(\mathbf{Z}, \mathbf{w}) = \mathbf{Z} \text{softmax}(0 \cdot \mathbf{Z}^T \mathbf{w} + \log(\mathbf{s})) = \frac{1}{S} \sum_{s=1}^S \mathbf{z}_s, \quad (28)$$

$$\boldsymbol{\mu} = \text{AttPool}_0(\tilde{\mathbf{Z}}, \mathbf{w}) = \tilde{\mathbf{Z}} \text{softmax}(0 \cdot \tilde{\mathbf{Z}}^T \mathbf{w} + \log(\tilde{\mathbf{s}})) = \frac{1}{N} \sum_{i=1}^N \frac{1}{S_i} \sum_{s=1}^S \mathbf{z}_{is} = \frac{1}{N} \sum_{i=1}^N \bar{\mathbf{z}}_i. \quad (29)$$

C Additional Algorithmic Details

C.1 AP-OOD Algorithmic Overview

Algorithm 1 AP-OOD

Require: $(\mathbf{x}_1, \dots, \mathbf{x}_N), \phi_e, \phi_d, \beta, M, \text{nsteps}$

- 1: **for** $i = 1$ to N **do**
- 2: Compute sequence embedding \mathbf{Z}_i using $\mathbf{Z}_i \leftarrow \phi_e(\mathbf{x}_i)$ or $\mathbf{Z}_i \leftarrow \phi_d(\phi_e(\mathbf{x}_i))$.
- 3: **for** step = 1 to nsteps **do**
- 4: Sample mini-batch $\{\mathbf{Z}_i\}_{i \in \mathcal{B}}$ with batch indices \mathcal{B} .
- 5: Form batch-local concatenation $\tilde{\mathbf{Z}}_B \leftarrow \|\mathbf{Z}_i\|_{i \in \mathcal{B}}$.
- 6: Compute loss $\mathcal{L} \leftarrow \frac{1}{|\mathcal{B}|} \sum_{i \in \mathcal{B}} d^2(\mathbf{Z}_i, \tilde{\mathbf{Z}}_B) - \sum_{j=1}^M \log(\|\mathbf{w}_j\|_2^2)$.
- 7: Compute gradients of \mathcal{L} w.r.t. $(\mathbf{w}_1, \dots, \mathbf{w}_M)$ and perform a gradient update
- 8: Form the concatenation of sequence representations $\tilde{\mathbf{Z}} \leftarrow (\mathbf{Z}_1 \| \dots \| \mathbf{Z}_N)$
- 9: $s(\mathbf{Z}) \leftarrow \sum_{j=1}^M -d_j^2(\mathbf{Z}, \tilde{\mathbf{Z}}) + \log(\|\mathbf{w}_j\|_2^2)$.
- 10: **return** $s(\cdot)$

C.2 Attention Pooling over the Corpus

In this section, we describe the process of performing attention pooling over a long sequence $\tilde{\mathbf{Z}}$ that is too large to fit into memory. For this, we need the log-sum-exponential function. We follow the notation from [Ramsauer et al. \(2021\)](#).

$$\text{lse}(\beta, \mathbf{a}) = \beta^{-1} \log \left(\sum_{s=1}^S \exp(\beta a_s) \right) \quad (30)$$

Algorithm 2 Attention pooling over a long sequence

Require: $\tilde{\mathbf{Z}} = (\tilde{\mathbf{z}}_1, \dots, \tilde{\mathbf{z}}_S) \in \mathbb{R}^{D \times S}, \beta, \mathbf{w}, B$

- 1: $E \leftarrow -\infty$
- 2: $\boldsymbol{\mu} \leftarrow \mathbf{0}$
- 3: **for** $s \leftarrow 1$ to S **step** B **do**
- 4: Load mini-batch $\mathbf{B} \leftarrow (\tilde{\mathbf{z}}_s, \dots, \tilde{\mathbf{z}}_{s+B})$
- 5: $E_B \leftarrow \text{lse}(\beta, \mathbf{B}^T \mathbf{w})$
- 6: $\mathbf{p} \leftarrow \exp(\beta(\mathbf{B}^T \mathbf{w} - E_B))$
- 7: $\boldsymbol{\mu}_B \leftarrow \mathbf{B} \mathbf{p}$
- 8: $p_B \leftarrow \sigma(\beta(E_B - E))$
- 9: $\boldsymbol{\mu} \leftarrow p_B \boldsymbol{\mu}_B + (1 - p_B) \boldsymbol{\mu}$
- 10: $E \leftarrow \beta^{-1} \log(\exp(\beta E_B) + \exp(\beta E))$
- 11: **return** $\boldsymbol{\mu}$

C.3 Extension: Multiple Queries per Head

We extend AP-OOD and use multiple queries per head. We use a set of stacked queries $\mathbf{W}_j = (\mathbf{w}_{j1}, \dots, \mathbf{w}_{jT}) \in \mathbb{R}^{D \times T}$ per head. For simplicity, we consider a single head with the queries \mathbf{W} for now. We begin by extending the softmax notation from [Ramsauer et al. \(2021\)](#) to matrix-valued arguments. Given a matrix $\mathbf{A} \in \mathbb{R}^{S \times T}$

$$\text{softmax}(\beta \mathbf{A})_{st} := \frac{\exp(\beta a_{st})}{\sum_{s'=1}^S \sum_{t'=1}^T \exp(\beta a_{s't'})}. \quad (31)$$

In other words, the softmax normalizes over the rows and columns of \mathbf{A} . Next, we extend the attention pooling process from Equation (7) with the matrix-valued softmax: AP-OOD transforms the sequence

representation $\mathbf{Z} \in \mathbb{R}^{D \times S}$ with S tokens to a new sequence representation $\bar{\mathbf{Z}} = \mathbf{Z}\mathbf{P} \in \mathbb{R}^{D \times T}$ with T tokens. The updated attention pooling process is

$$\text{AttPool}_\beta(\mathbf{Z}, \mathbf{W}) := \mathbf{Z} \text{softmax}(\beta \mathbf{Z}^T \mathbf{W}) \quad \text{and} \quad \bar{\mathbf{Z}} := \text{AttPool}_\beta(\mathbf{Z}, \mathbf{W}). \quad (32)$$

Finally, AP-OOD uses $\mathbf{W} \in \mathbb{R}^{D \times T}$ to transform the $\bar{\mathbf{Z}} \in \mathbb{R}^{D \times T}$ to a real number with the Frobenius inner product $\langle \mathbf{W}, \bar{\mathbf{Z}} \rangle_F = \text{vec}(\mathbf{W})^T \text{vec}(\bar{\mathbf{Z}}) = \text{Tr}(\mathbf{W}^T \bar{\mathbf{Z}})$. To summarize, the extended squared distance is

$$d^2(\mathbf{Z}, \bar{\mathbf{Z}}) := \sum_{j=1}^M \left(\text{Tr}(\mathbf{W}_j^T \mathbf{Z} \text{softmax}(\beta \mathbf{Z}^T \mathbf{W}_j)) - \text{Tr}(\mathbf{W}_j^T \bar{\mathbf{Z}} \text{softmax}(\beta \bar{\mathbf{Z}}^T \mathbf{W}_j)) \right)^2. \quad (33)$$

Finally, the regularizing term is $-\log(\|\mathbf{W}\|_F^2)$ (where $\|\cdot\|_F^2$ denotes the squared Frobenius norm). To summarize, the extended loss is

$$\mathcal{L}(\mathbf{W}_1, \dots, \mathbf{W}_M) := \frac{1}{N} \sum_{i=1}^N d^2(\mathbf{Z}_i, \bar{\mathbf{Z}}) - \sum_{j=1}^M \log(\|\mathbf{W}_j\|_F^2). \quad (34)$$

Table 3: Unsupervised OOD detection performance on English-to-French translation. We compare results from AP-OOD, Mahalanobis (Lee et al., 2018; Ren et al., 2023), KNN (Sun et al., 2022), Deep SVDD (Ruff et al., 2018), model perplexity (Ren et al., 2023), and entropy (Malinin & Gales, 2020) on a Transformer (base) trained on WMT15 En–Fr as the ID data set. ↓ indicates “lower is better” and ↑ “higher is better”. All values in %. We estimate standard deviations across five independent data set splits and training runs.

	IT	Koran	Law	Medical	Subtitles	ndd2015	ndt2015	nt2014	Mean
Input OOD									
Mahalanobis	AUROC ↑	93.94 \pm 0.01	66.82 \pm 0.29	49.39 \pm 0.30	78.50 \pm 0.41	89.61\pm0.09	65.87 \pm 0.01	66.44 \pm 0.01	51.53 \pm 0.01
	FPR95 ↓	31.29\pm0.29	93.46\pm0.27	91.26\pm0.50	63.13\pm0.77	59.60\pm0.48	87.01 \pm 0.14	89.09 \pm 0.10	97.13\pm0.10
KNN	AUROC ↑	94.16 \pm 0.01	66.16 \pm 0.24	46.68 \pm 0.22	79.62 \pm 0.41	89.16 \pm 0.11	64.81 \pm 0.05	65.63 \pm 0.05	53.21 \pm 0.05
	FPR95 ↓	32.44 \pm 0.12	94.69 \pm 0.28	92.71 \pm 0.34	67.04 \pm 0.73	63.35 \pm 0.32	88.91 \pm 0.07	89.97 \pm 0.04	97.51 \pm 0.03
Deep SVDD	AUROC ↑	92.53 \pm 0.15	64.12 \pm 0.81	51.56\pm1.21	77.40 \pm 0.52	87.64 \pm 0.37	63.30 \pm 0.40	63.58 \pm 0.31	49.31 \pm 0.31
	FPR95 ↓	39.37 \pm 0.94	95.24 \pm 0.28	92.80 \pm 0.29	66.17 \pm 0.71	65.53 \pm 1.33	89.87 \pm 0.22	90.91 \pm 0.27	98.07 \pm 0.19
AP-OOD (Ours)	AUROC ↑	94.88\pm0.08	73.51\pm0.33	51.11\pm0.38	81.80\pm0.35	89.14 \pm 0.32	69.98\pm0.15	70.40\pm0.27	57.82\pm0.23
	FPR95 ↓	25.00\pm0.59	87.48\pm0.33	89.45\pm0.67	58.51\pm0.60	60.78 \pm 2.07	86.45\pm0.91	87.05\pm0.32	94.19 \pm 0.41
Output OOD									
Perplexity	AUROC ↑	94.06 \pm 0.00	77.05 \pm 0.20	45.18 \pm 0.38	75.41 \pm 0.42	92.38\pm0.08	75.32 \pm 0.02	75.81\pm0.02	61.74 \pm 0.02
	FPR95 ↓	35.36 \pm 0.01	90.54 \pm 0.35	90.14\pm0.34	69.17 \pm 0.60	50.11\pm0.58	83.94 \pm 0.04	85.47 \pm 0.00	96.80 \pm 0.00
Entropy	AUROC ↑	71.44 \pm 0.22	86.14\pm0.32	53.98 \pm 0.23	51.12 \pm 0.44	70.95 \pm 0.47	75.11 \pm 0.96	72.96 \pm 0.22	71.31\pm0.17
	FPR95 ↓	71.19 \pm 0.95	56.19\pm1.91	93.94 \pm 0.37	90.27 \pm 0.64	74.56 \pm 1.23	76.28\pm2.13	77.65\pm1.54	85.71 \pm 1.32
Mahalanobis	AUROC ↑	90.74 \pm 0.01	69.38 \pm 0.17	52.25 \pm 0.14	75.68 \pm 0.47	86.57 \pm 0.08	62.28 \pm 0.03	62.76 \pm 0.02	48.63 \pm 0.02
	FPR95 ↓	57.02 \pm 0.44	94.26 \pm 0.23	97.15 \pm 0.15	81.34 \pm 0.33	76.16 \pm 0.79	93.09 \pm 0.29	93.93 \pm 0.13	98.00 \pm 0.09
KNN	AUROC ↑	95.35 \pm 0.04	71.55 \pm 0.17	57.40\pm0.14	78.53\pm0.58	87.06 \pm 0.12	67.16 \pm 0.12	67.90 \pm 0.13	58.38 \pm 0.10
	FPR95 ↓	27.61 \pm 0.31	94.13 \pm 0.11	93.82 \pm 0.32	65.10 \pm 0.58	72.73 \pm 0.43	91.33 \pm 0.08	91.88 \pm 0.10	96.79 \pm 0.05
Deep SVDD	AUROC ↑	89.20 \pm 0.13	67.28 \pm 0.80	54.40 \pm 0.83	73.96 \pm 0.65	84.00 \pm 0.19	60.37 \pm 0.57	60.66 \pm 0.37	47.11 \pm 0.22
	FPR95 ↓	62.41 \pm 1.21	95.19 \pm 0.48	95.03 \pm 0.65	81.50 \pm 1.69	81.56 \pm 1.15	93.93 \pm 0.26	95.75 \pm 0.44	98.41 \pm 0.16
AP-OOD (Ours)	AUROC ↑	96.28\pm0.11	80.70 \pm 0.50	53.07 \pm 0.68	80.84\pm0.87	93.88\pm0.36	80.64\pm0.57	81.39\pm0.56	68.12 \pm 0.65
	FPR95 ↓	21.20\pm0.65	82.49 \pm 1.29	87.38\pm0.44	63.67\pm1.03	40.27 \pm 3.02	77.14 \pm 1.68	78.39 \pm 1.29	94.50 \pm 0.40

Table 4: Supervised OOD detection performance on English-to-French translation. We compare results from AP-OOD, binary logits, relative mahalanobis (Ren et al., 2023), and Deep SAD (Ruff et al., 2019) on a Transformer (base) trained on WMT15 En–Fr as the ID data set. ↓ indicates “lower is better” and ↑ “higher is better”. All values in %. We estimate standard deviations across five independent data set splits and training runs.

	IT	Koran	Law	Medical	Subtitles	ndd2015	ndt2015	nt2014	Mean
Input OOD									
Binary logits	AUROC ↑	93.60 \pm 0.34	95.17\pm0.05	54.29 \pm 0.33	70.47 \pm 0.67	90.53 \pm 0.46	89.91 \pm 0.15	89.80\pm0.16	85.65\pm0.06
	FPR95 ↓	28.58 \pm 1.19	34.91\pm0.75	97.16 \pm 0.06	82.27 \pm 0.64	41.03 \pm 0.96	60.64 \pm 0.41	57.56\pm0.58	75.78 \pm 0.44
Relative Mahalanobis	AUROC ↑	92.82 \pm 0.26	93.31 \pm 0.09	43.07 \pm 0.38	74.40\pm0.40	95.73\pm0.21	89.33 \pm 0.04	88.88 \pm 0.05	82.06 \pm 0.13
	FPR95 ↓	19.27\pm0.44	53.50 \pm 0.68	94.27\pm0.24	67.63\pm0.66	13.38\pm0.28	59.06 \pm 0.43	61.49 \pm 0.37	83.24 \pm 0.14
Deep SAD	AUROC ↑	94.56\pm0.13	94.77 \pm 0.14	57.44\pm0.58	71.67 \pm 0.27	91.57 \pm 0.21	90.07 \pm 0.16	89.47 \pm 0.12	84.42 \pm 0.19
	FPR95 ↓	28.31\pm0.62	40.77 \pm 1.35	97.10 \pm 0.13	83.74 \pm 0.28	41.15 \pm 1.24	61.54 \pm 0.81	62.11 \pm 0.82	79.33 \pm 0.65
AP-OOD (Ours)	AUROC ↑	94.97\pm0.54	96.17\pm0.35	56.82 \pm 1.03	79.31\pm0.99	95.03 \pm 0.41	90.66 \pm 0.39	90.73\pm0.36	86.56\pm0.36
	FPR95 ↓	29.93 \pm 2.86	26.04\pm2.97	94.46 \pm 0.83	79.06 \pm 1.44	29.17 \pm 2.32	56.34\pm2.46	55.12 \pm 1.47	69.75 \pm 1.36
Output OOD									
Binary logits	AUROC ↑	95.15 \pm 0.06	95.64 \pm 0.17	58.96\pm0.79	74.70 \pm 0.37	92.79 \pm 0.22	90.32 \pm 0.19	90.21 \pm 0.16	85.73\pm0.12
	FPR95 ↓	27.58 \pm 0.44	30.49 \pm 1.89	96.36 \pm 0.28	82.09 \pm 0.61	39.08 \pm 1.07	57.36\pm0.95	57.65 \pm 0.68	75.34 \pm 0.41
Relative Mahalanobis	AUROC ↑	92.83 \pm 0.18	94.94 \pm 0.14	41.88 \pm 0.42	71.09 \pm 0.27	95.14 \pm 0.16	88.86 \pm 0.02	87.83 \pm 0.08	82.59 \pm 0.10
	FPR95 ↓	28.72 \pm 0.40	36.30 \pm 1.18	95.54\pm0.29	80.88\pm0.20	20.42\pm0.57	67.39 \pm 0.52	67.80 \pm 0.48	85.74 \pm 0.20
Deep SAD	AUROC ↑	95.88\pm0.13	96.57 \pm 0.21	56.47 \pm 1.31	76.35 \pm 0.60	94.79 \pm 0.12	90.66\pm0.11	90.40\pm0.11	86.21\pm0.18
	FPR95 ↓	23.73\pm0.47	21.38 \pm 1.75	95.86 \pm 0.38	82.47 \pm 0.52	30.23 \pm 0.82	58.14 \pm 1.45	57.37\pm1.64	75.73 \pm 0.23
AP-OOD (Ours)	AUROC ↑	95.82 \pm 0.24	96.85\pm0.24	59.22\pm0.92	78.27\pm1.67	95.78\pm0.13	90.31 \pm 0.33	89.87 \pm 0.35	83.97 \pm 0.90
	FPR95 ↓	28.51 \pm 1.44	19.94 \pm 1.78	93.65\pm0.36	81.37 \pm 0.56	26.96 \pm 1.04	59.28 \pm 1.36	57.48\pm1.09	73.64\pm1.21

D Experiments

D.1 Translation

We train a Transformer (base) on WMT15 En–Fr (Bojar et al., 2015). The model trains for 100,000 steps using AdamW (Loshchilov & Hutter, 2017) with a cosine schedule (Loshchilov & Hutter, 2016), linear warmup, and a peak learning rate of 5×10^{-4} . We set the batch size to 1024 and the context length to 512. Following Ren et al. (2023), the AUX data set is ParaCrawl En–Fr, and the OOD data sets are newstest2014 (nt2014), newsdiscussdev2015 (ndd2015), and newsdiscussstest2015 (ndt2015) from WMT15 (Bojar et al., 2015), and the Law, Koran, Medical, IT, and Subtitles subsets from OPUS (Tiedemann, 2012; Aulamo & Tiedemann, 2019).

Table 3 shows the results on unsupervised OOD detection on the translation task. AP-OOD gives the best average results for the input and output settings. It is noteworthy that in the translation task, the

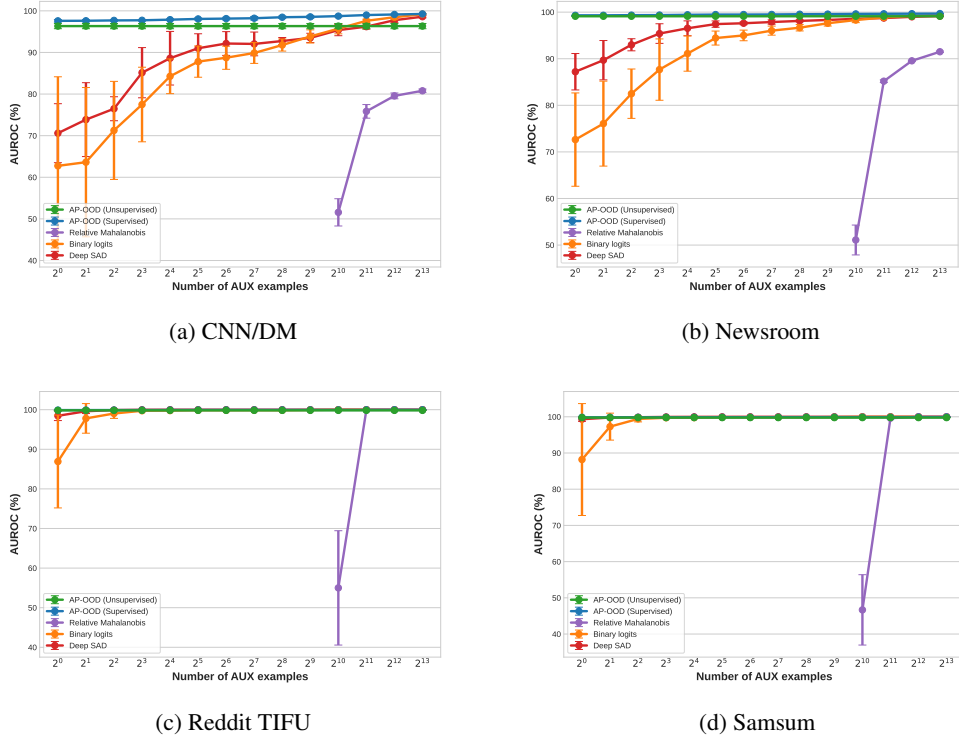


Figure 4: OOD detection performance on text summarization for all OOD data sets. We vary the number of AUX examples and compare results from AP-OOD, binary logits (Ren et al., 2023), relative Mahalanobis (Ren et al., 2023), and Deep SAD (Ruff et al., 2019).

prediction-based methods perform better, with the perplexity baseline outperforming all embedding-based methods evaluated on the output token embeddings except AP-OOD. We hypothesize that this discrepancy can be explained as follows: In translation, ID uncertainty is typically low because the source sentence largely dictates what must be generated — specific words, names, and inflections — so ID perplexities are small and tightly clustered. In text summarization, ID uncertainty is higher because many different summaries can be equally valid, with freedom in what to include and how to phrase it. This raises and spreads ID perplexity and weakens ID–OOD separation when using perplexity.

In the fully supervised setting, we train all methods on the embeddings of 100,000 ID embeddings and 100,000 AUX embeddings obtained from a Transformer (base) trained on WMT15 En–Fr translation. Table 4 shows that AP-OOD improves supervised OOD detection results w.r.t. the mean AUROC and FPR95 metrics.

D.2 Additional Experiments on Text Summarization

In the fully supervised setting, we train all methods on the embeddings of 100,000 ID examples and 10,000 AUX examples obtained from PEGASUS_{LARGE} trained on text summarization using the XSUM data set. Table 5 shows that AP-OOD substantially improves fully supervised OOD detection results, improving the previously best mean FPR95 of 1.06% (binary logits) to 0.28% in the input OOD setting. Figure 4 shows the results for the semi-supervised setting when scaling the number of AUX examples on all OOD data sets for text summarization. We evaluate relative Mahalanobis only for $N' \geq 1024$, because Σ is not invertible when using fewer AUX examples. In contrast to Figure 3, Figure 4 also shows the results for Reddit TIFU and Samsum. On these two data sets, all evaluated methods except relative Mahalanobis achieve near-perfect OOD detection results for $N' \geq 8$.

Table 5: Supervised OOD detection performance on text summarization. We compare results from AP-OOD, binary logits (Ren et al., 2023), relative Mahalanobis (Ren et al., 2023), and Deep SAD (Ruff et al., 2019) on PEGASUS_{LARGE} trained on XSUM as the ID data set. ↓ indicates “lower is better” and ↑ “higher is better”. All values in %. We estimate standard deviations across five independent data set splits and training runs.

		CNN/DM	Newsroom	Reddit	Samsun	Mean
Input OOD						
Binary logits	AUROC ↑	99.43 \pm 0.11	99.52 \pm 0.06	100.00 \pm 0.00	99.99 \pm 0.00	99.73
	FPR95 ↓	2.32 \pm 0.59	1.93 \pm 0.17	0.00 \pm 0.00	0.01 \pm 0.01	1.06
Relative Mahalanobis	AUROC ↑	81.28 \pm 0.19	91.85 \pm 0.20	99.96 \pm 0.00	99.98 \pm 0.00	93.27
	FPR95 ↓	62.92 \pm 0.34	28.22 \pm 0.43	0.00 \pm 0.01	0.01 \pm 0.01	22.79
Deep SAD	AUROC ↑	98.85 \pm 0.17	99.24 \pm 0.07	100.00 \pm 0.00	100.00 \pm 0.00	99.52
	FPR95 ↓	3.69 \pm 0.81	2.38 \pm 0.16	0.00 \pm 0.00	0.00 \pm 0.00	1.52
AP-OOD (Ours)	AUROC ↑	99.83 \pm 0.18	99.71 \pm 0.05	100.00 \pm 0.00	100.00 \pm 0.00	99.88
	FPR95 ↓	0.37 \pm 0.51	0.76 \pm 0.19	0.00 \pm 0.00	0.00 \pm 0.00	0.28
Output OOD						
Binary logits	AUROC ↑	98.67 \pm 0.26	99.49 \pm 0.03	99.99 \pm 0.01	99.94 \pm 0.02	99.52
	FPR95 ↓	5.01 \pm 0.97	1.77 \pm 0.07	0.00 \pm 0.00	0.09 \pm 0.04	1.72
Relative Mahalanobis	AUROC ↑	93.58 \pm 0.18	97.41 \pm 0.08	99.82 \pm 0.01	99.54 \pm 0.03	97.59
	FPR95 ↓	24.32 \pm 0.33	8.54 \pm 0.23	0.04 \pm 0.01	1.00 \pm 0.09	8.47
Deep SAD	AUROC ↑	98.39 \pm 0.23	99.53 \pm 0.03	100.00 \pm 0.00	99.96 \pm 0.00	99.47
	FPR95 ↓	6.00 \pm 0.75	1.66 \pm 0.14	0.00 \pm 0.00	0.07 \pm 0.03	1.93
AP-OOD (Ours)	AUROC ↑	99.00 \pm 0.13	99.59 \pm 0.02	100.00 \pm 0.00	99.98 \pm 0.00	99.64
	FPR95 ↓	3.25 \pm 0.42	1.24 \pm 0.07	0.00 \pm 0.00	0.01 \pm 0.01	1.13

D.3 Toy Experiment

Toy experiment. We present a toy experiment illustrating the main intuitions behind AP-OOD. Figure 1 demonstrates a simple failure mode of mean pooling approaches: First, we generate ID and OOD token embeddings $Z_i \in \mathbb{R}^{2 \times 2}$. Each ID sequence representation consists of one token sampled from $\mathcal{N}((1, 1), \sigma^2 I)$ and one token sampled from $\mathcal{N}((-1, -1), \sigma^2 I)$. The OOD sequences contain two tokens sampled from $\mathcal{N}((-1, 1), \sigma^2 I)$ and $\mathcal{N}((1, -1), \sigma^2 I)$, respectively. We set $\sigma := 0.1$. The left panel shows the generated sequences, where each sequence consists of two dots (representing the two tokens) connected by a line. Because the means of the ID and OOD sequences both cluster around the origin (central panel), the Mahalanobis distance with mean pooling fails to discriminate between them (right panel). Figure 2 shows how AP-OOD overcomes this limitation: We set $M = 1$ and $T = 1$ and train AP-OOD as described in Section 2.1 on the ID data only, but we modify the pooling mechanism from Equation (7): We replace the dot product similarity in the softmax with the negative squared Euclidean distance, as it is known to work better in low-dimensional spaces. Formally, we modify the attention pooling process from Equation 7 as follows:

$$\text{AttPool}_\beta(Z, w) := \sum_{s=1}^S z_s \frac{\exp(-\frac{\beta}{2} \|z_s - w\|_2^2)}{\sum_{s'=1}^S \exp(-\frac{\beta}{2} \|z_{s'} - w\|_2^2)}. \quad (35)$$

The left panel of Figure 2 shows that the loss landscape of w forms two basins at the locations of the ID tokens. The central panel shows that after training, w is located in one of the basins. Finally, the right panel shows that AP-OOD perfectly discriminates ID and OOD.

D.4 Hyperparameter selection.

To find the values for β , M , and T in the unsupervised setting, we perform a grid search using the values $\beta \in \{\frac{1}{\sqrt{D}}, 0.25, 0.5, 1, 2\}$ and $T \in \{1, 4, 16\}$. We select M such that the total number of parameters of AP-OOD equals the number of entries in Σ of the Mahalanobis method, i.e., such that $MT = D$. We select the hyperparameter configuration by evaluating each resulting model on OOD detection using a validation split of the AUX data set (in the unsupervised setting, we use the AUX data set only for model selection, not for training the model), and we select the model with the highest AUROC. In the supervised setting, we follow the same procedure, and we additionally select $\lambda \in \{0.1, 1, 10\}$.

Table 6: Unsupervised OOD detection performance on text summarization. We compare results from AP-OOD when using $s(\mathbf{Z})$ and $s_{\min}(\mathbf{Z})$, on PEGASUS_{LARGE} trained on XSUM as the ID data set. \downarrow indicates “lower is better” and \uparrow “higher is better”. All values in %. We estimate standard deviations across five independent dataset splits and training runs.

	CNN/DM	Newsroom	Reddit	Samsun	Mean
Input OOD					
$s(\mathbf{Z})$	AUROC \uparrow 96.13\pm0.44	99.10\pm0.08	99.91\pm0.03	99.80\pm0.04	98.74
	FPR95 \downarrow 19.51 \pm 2.24	4.11 \pm 0.28	0.00 \pm 0.01	0.04 \pm 0.03	5.91
$s_{\min}(\mathbf{Z})$	AUROC \uparrow 96.08 \pm 0.37	97.48 \pm 0.28	99.71 \pm 0.20	97.67 \pm 0.35	97.74
	FPR95 \downarrow 18.78\pm2.73	11.16 \pm 1.21	0.01 \pm 0.01	12.04 \pm 3.04	10.50
Output OOD					
$s(\mathbf{Z})$	AUROC \uparrow 93.37 \pm 0.54	92.62\pm0.67	98.04\pm0.28	98.30\pm0.11	95.59
	FPR95 \downarrow 23.12\pm1.97	29.91\pm2.93	6.34\pm1.56	6.83\pm0.64	16.55
$s_{\min}(\mathbf{Z})$	AUROC \uparrow 93.82\pm1.56	88.30 \pm 3.45	95.94 \pm 2.25	90.13 \pm 4.31	92.05
	FPR95 \downarrow 26.60 \pm 5.53	38.26 \pm 3.73	18.49 \pm 9.01	36.71 \pm 12.40	30.02

Table 7: Unsupervised OOD detection performance on text summarization. We compare results from AP-OOD trained on XSUM as the ID data set when varying β . \downarrow indicates “lower is better” and \uparrow “higher is better”. All values in %. We estimate standard deviations across five independent dataset splits and training runs.

	CNN/DM	Newsroom	Reddit	Samsun	Mean
Input OOD					
$\beta = 0$	AUROC \uparrow 66.83 \pm 0.44	81.42 \pm 0.27	94.81 \pm 0.32	93.38 \pm 0.20	84.11
	FPR95 \downarrow 97.17 \pm 0.10	76.31 \pm 0.35	41.12 \pm 3.42	19.96 \pm 0.84	58.64
$\beta = 0.25$	AUROC \uparrow 97.76\pm0.11	98.75 \pm 0.07	99.87\pm0.06	99.46 \pm 0.09	98.96
	FPR95 \downarrow 11.07\pm0.74	4.75\pm0.41	0.00\pm0.00	0.02 \pm 0.02	3.96
$\beta = 0.5$	AUROC \uparrow 96.13\pm0.44	99.10\pm0.08	99.91\pm0.03	99.80 \pm 0.04	98.74
	FPR95 \downarrow 19.51\pm2.24	4.11\pm0.28	0.00 \pm 0.01	0.04 \pm 0.03	5.91
$\beta = 1$	AUROC \uparrow 91.36 \pm 0.41	98.77 \pm 0.05	99.75 \pm 0.02	99.83 \pm 0.01	97.43
	FPR95 \downarrow 38.78 \pm 4.50	4.94 \pm 0.23	0.02 \pm 0.02	0.00\pm0.00	10.94
$\beta = 2$	AUROC \uparrow 84.29 \pm 0.91	97.58 \pm 0.09	99.52 \pm 0.05	99.76 \pm 0.01	95.28
	FPR95 \downarrow 63.31 \pm 4.63	9.14 \pm 0.46	0.12 \pm 0.07	0.05 \pm 0.03	18.16
$\beta = 1/\sqrt{D}$	AUROC \uparrow 89.09 \pm 0.66	90.59 \pm 0.35	99.59 \pm 0.18	99.87\pm0.01	94.79
	FPR95 \downarrow 53.96 \pm 3.30	47.50 \pm 1.83	0.17 \pm 0.18	0.04 \pm 0.02	25.42
Output OOD					
$\beta = 0$	AUROC \uparrow 77.67 \pm 1.37	85.10 \pm 0.61	84.12 \pm 1.08	91.70 \pm 0.44	84.65
	FPR95 \downarrow 82.07 \pm 1.30	69.32 \pm 1.65	57.30 \pm 1.73	29.37 \pm 1.73	59.52
$\beta = 0.25$	AUROC \uparrow 91.37 \pm 0.64	93.66\pm0.13	94.79 \pm 0.29	96.56 \pm 0.27	94.10
	FPR95 \downarrow 43.03 \pm 1.71	34.70 \pm 0.32	38.38 \pm 3.27	18.61 \pm 2.44	33.68
$\beta = 0.5$	AUROC \uparrow 93.37\pm0.54	92.62\pm0.67	98.04\pm0.28	98.30\pm0.11	95.59
	FPR95 \downarrow 23.12\pm1.97	29.91\pm2.93	6.34\pm1.56	6.83\pm0.64	16.55
$\beta = 1$	AUROC \uparrow 93.06 \pm 0.57	91.82 \pm 0.71	97.66 \pm 0.33	97.91 \pm 0.22	95.11
	FPR95 \downarrow 24.04 \pm 1.95	32.04 \pm 2.97	9.29 \pm 1.71	8.82 \pm 1.42	18.55
$\beta = 2$	AUROC \uparrow 93.25\pm0.48	91.98 \pm 0.73	97.57 \pm 0.40	97.97\pm0.19	95.19
	FPR95 \downarrow 23.69\pm1.94	31.23\pm3.09	10.06 \pm 2.44	8.37 \pm 1.30	18.34
$\beta = 1/\sqrt{D}$	AUROC \uparrow 54.67 \pm 0.72	80.59 \pm 0.72	94.12 \pm 0.30	94.93 \pm 0.35	81.08
	FPR95 \downarrow 92.40 \pm 0.21	65.83 \pm 1.03	30.04 \pm 1.15	27.20 \pm 1.94	53.87

D.5 OOD score comparison

We experimentally compare the min-based OOD score $s_{\min}(\mathbf{Z})$ and its upper bound $s(\mathbf{Z})$. For training, we use the loss from Equation (10) in both settings. The results in Table 6 show that $s(\mathbf{Z})$ achieves better OOD discrimination w.r.t. the mean AUROC and FPR95. While $s_{\min}(\mathbf{Z})$ roughly matches the OOD detection metrics of $s(\mathbf{Z})$ on CNN/DM for both input and output, $s_{\min}(\mathbf{Z})$ lags behind $s(\mathbf{Z})$ on the other OOD data sets.

Table 8: Unsupervised OOD detection performance on text summarization. We compare results from AP-OOD trained on XSUM as the ID data set when varying M and T . \downarrow indicates “lower is better” and \uparrow “higher is better”. All values in %. We estimate standard deviations across five independent dataset splits and training runs.

	CNN/DM	Newsroom	Reddit	Samsun	Mean
Input OOD					
$M = 1024 \quad T = 1$	AUROC \uparrow FPR95 \downarrow	$97.16^{\pm 0.22}$ $14.72^{\pm 0.83}$	$98.25^{\pm 0.11}$ $7.54^{\pm 0.62}$	$99.82^{\pm 0.01}$ $\underline{0.00^{\pm 0.00}}$	$99.32^{\pm 0.03}$ $0.64^{\pm 0.11}$
$M = 512 \quad T = 2$	AUROC \uparrow FPR95 \downarrow	$97.98^{\pm 0.16}$ $9.77^{\pm 0.80}$	$98.83^{\pm 0.07}$ $4.67^{\pm 0.30}$	$99.87^{\pm 0.03}$ $\underline{0.00^{\pm 0.00}}$	$99.60^{\pm 0.04}$ $0.02^{\pm 0.02}$
$M = 256 \quad T = 4$	AUROC \uparrow FPR95 \downarrow	$97.76^{\pm 0.11}$ $11.07^{\pm 0.74}$	$98.75^{\pm 0.07}$ $4.75^{\pm 0.41}$	$99.87^{\pm 0.06}$ $\underline{0.00^{\pm 0.00}}$	$99.46^{\pm 0.09}$ $0.02^{\pm 0.02}$
$M = 128 \quad T = 8$	AUROC \uparrow FPR95 \downarrow	$97.53^{\pm 0.15}$ $12.48^{\pm 1.14}$	$98.49^{\pm 0.15}$ $5.94^{\pm 0.65}$	$99.83^{\pm 0.07}$ $\underline{0.00^{\pm 0.00}}$	$99.14^{\pm 0.12}$ $0.25^{\pm 0.10}$
$M = 64 \quad T = 16$	AUROC \uparrow FPR95 \downarrow	$97.10^{\pm 0.09}$ $14.30^{\pm 0.77}$	$98.14^{\pm 0.16}$ $7.87^{\pm 0.86}$	$99.84^{\pm 0.07}$ $0.00^{\pm 0.00}$	$98.81^{\pm 0.16}$ $0.99^{\pm 0.50}$
$M = 32 \quad T = 32$	AUROC \uparrow FPR95 \downarrow	$96.84^{\pm 0.35}$ $14.97^{\pm 1.96}$	$97.78^{\pm 0.15}$ $10.18^{\pm 0.80}$	$99.83^{\pm 0.05}$ $0.01^{\pm 0.02}$	$98.56^{\pm 0.28}$ $2.53^{\pm 2.12}$
$M = 16 \quad T = 64$	AUROC \uparrow FPR95 \downarrow	$96.23^{\pm 0.45}$ $16.65^{\pm 1.99}$	$97.35^{\pm 0.24}$ $12.55^{\pm 1.15}$	$99.73^{\pm 0.11}$ $0.09^{\pm 0.20}$	$98.19^{\pm 0.24}$ $5.69^{\pm 1.87}$
$M = 8 \quad T = 128$	AUROC \uparrow FPR95 \downarrow	$95.56^{\pm 0.38}$ $18.16^{\pm 1.57}$	$96.47^{\pm 0.46}$ $16.34^{\pm 1.91}$	$99.67^{\pm 0.27}$ $0.52^{\pm 1.13}$	$97.44^{\pm 0.25}$ $11.29^{\pm 1.78}$
$M = 4 \quad T = 256$	AUROC \uparrow FPR95 \downarrow	$94.58^{\pm 0.67}$ $20.10^{\pm 2.32}$	$94.75^{\pm 0.52}$ $21.71^{\pm 2.30}$	$99.27^{\pm 0.86}$ $2.01^{\pm 4.09}$	$95.24^{\pm 0.25}$ $24.58^{\pm 1.83}$
$M = 2 \quad T = 512$	AUROC \uparrow FPR95 \downarrow	$93.17^{\pm 0.75}$ $22.86^{\pm 2.20}$	$91.87^{\pm 0.56}$ $27.09^{\pm 1.48}$	$98.43^{\pm 2.39}$ $4.95^{\pm 9.38}$	$89.87^{\pm 0.86}$ $39.75^{\pm 3.06}$
$M = 1 \quad T = 1024$	AUROC \uparrow FPR95 \downarrow	$90.90^{\pm 1.20}$ $27.14^{\pm 3.03}$	$88.10^{\pm 0.83}$ $32.64^{\pm 2.29}$	$96.68^{\pm 5.76}$ $9.03^{\pm 16.78}$	$81.41^{\pm 1.06}$ $52.73^{\pm 3.76}$
Output OOD					
$M = 1024 \quad T = 1$	AUROC \uparrow FPR95 \downarrow	$92.47^{\pm 0.48}$ $39.11^{\pm 1.81}$	$94.17^{\pm 0.30}$ $34.69^{\pm 0.85}$	$98.36^{\pm 0.22}$ $3.11^{\pm 1.16}$	$97.77^{\pm 0.14}$ $12.59^{\pm 0.90}$
$M = 512 \quad T = 2$	AUROC \uparrow FPR95 \downarrow	$93.79^{\pm 0.25}$ $32.45^{\pm 1.29}$	$95.85^{\pm 0.18}$ $20.10^{\pm 0.67}$	$99.02^{\pm 0.20}$ $0.95^{\pm 0.66}$	$98.96^{\pm 0.06}$ $2.77^{\pm 0.54}$
$M = 256 \quad T = 4$	AUROC \uparrow FPR95 \downarrow	$93.35^{\pm 0.46}$ $33.67^{\pm 2.77}$	$95.48^{\pm 0.28}$ $21.73^{\pm 0.82}$	$99.19^{\pm 0.26}$ $\underline{0.86^{\pm 0.95}}$	$99.05^{\pm 0.06}$ $2.72^{\pm 0.52}$
$M = 128 \quad T = 8$	AUROC \uparrow FPR95 \downarrow	$93.24^{\pm 0.34}$ $32.84^{\pm 1.75}$	$95.27^{\pm 0.37}$ $23.40^{\pm 1.53}$	$99.21^{\pm 0.41}$ $0.99^{\pm 1.56}$	$98.99^{\pm 0.04}$ $3.26^{\pm 0.42}$
$M = 64 \quad T = 16$	AUROC \uparrow FPR95 \downarrow	$92.95^{\pm 0.82}$ $34.08^{\pm 4.22}$	$94.92^{\pm 0.39}$ $25.53^{\pm 1.87}$	$99.11^{\pm 0.36}$ $1.48^{\pm 1.63}$	$98.89^{\pm 0.14}$ $4.10^{\pm 0.70}$
$M = 32 \quad T = 32$	AUROC \uparrow FPR95 \downarrow	$92.54^{\pm 0.61}$ $37.21^{\pm 3.76}$	$94.11^{\pm 0.47}$ $29.56^{\pm 2.71}$	$98.67^{\pm 0.73}$ $4.68^{\pm 4.39}$	$98.63^{\pm 0.41}$ $6.11^{\pm 2.55}$
$M = 16 \quad T = 64$	AUROC \uparrow FPR95 \downarrow	$91.26^{\pm 1.17}$ $41.96^{\pm 4.43}$	$92.62^{\pm 1.40}$ $35.78^{\pm 5.78}$	$97.99^{\pm 2.33}$ $8.75^{\pm 13.44}$	$98.58^{\pm 0.84}$ $6.19^{\pm 4.88}$
$M = 8 \quad T = 128$	AUROC \uparrow FPR95 \downarrow	$90.94^{\pm 1.97}$ $41.24^{\pm 8.00}$	$91.99^{\pm 1.88}$ $36.42^{\pm 7.58}$	$97.10^{\pm 2.54}$ $13.13^{\pm 13.35}$	$98.28^{\pm 0.80}$ $7.58^{\pm 3.85}$
$M = 4 \quad T = 256$	AUROC \uparrow FPR95 \downarrow	$89.62^{\pm 1.80}$ $47.52^{\pm 9.04}$	$90.35^{\pm 2.64}$ $41.77^{\pm 12.21}$	$95.91^{\pm 3.26}$ $18.53^{\pm 16.24}$	$97.73^{\pm 0.96}$ $10.02^{\pm 4.76}$
$M = 2 \quad T = 512$	AUROC \uparrow FPR95 \downarrow	$87.82^{\pm 2.50}$ $52.18^{\pm 9.71}$	$88.06^{\pm 1.29}$ $50.66^{\pm 5.51}$	$94.00^{\pm 3.38}$ $28.44^{\pm 17.40}$	$96.91^{\pm 1.26}$ $13.98^{\pm 6.18}$
$M = 1 \quad T = 1024$	AUROC \uparrow FPR95 \downarrow	$86.45^{\pm 1.86}$ $50.92^{\pm 8.94}$	$86.95^{\pm 1.79}$ $49.61^{\pm 6.70}$	$93.43^{\pm 2.35}$ $29.61^{\pm 8.37}$	$96.10^{\pm 1.59}$ $14.82^{\pm 3.62}$

D.6 Ablations

Beta sensitivity analysis. We evaluate AP-OOD when varying the hyperparameter β on the summarization task. We select β from $\{0, 1/\sqrt{D}, 0.25, 0.5, 1, 2\}$, and we leave the settings for M and T unchanged (i.e., they are identical to the settings used in Table 1). Table 7 shows that AP-OOD on text summarization is relatively insensitive to the selection of β inside the range $[0.25, 2]$ in the input and output settings.

Number of heads M and queries T . We ablate on the number of heads M and the number of queries T of AP-OOD on the summarization task. For this ablation, we select $T \in \{1, 2, 4, 8, 16, 32, 64, 128, 512, 1024\}$ and we then select M such that the total number of parameters of AP-OOD equals the number of entries in Σ of the Mahalanobis method, i.e., such that $MT = D$. The results in Table 8 show that AP-OOD works best on the summarization task for both input and output when $M = 512$ and $T = 2$. Although the performance drops when decreasing M and increasing T , we find that AP-OOD is relatively insensitive to the number of heads and queries.

Table 9: Unsupervised OOD detection performance on text summarization. We compare results from AP-OOD trained on XSUM as the ID data set when using the dot product and the Euclidean similarity. ↓ indicates “lower is better” and ↑ “higher is better”. All values in %. We estimate standard deviations across five independent dataset splits and training runs.

		CNN/DM	Newsroom	Reddit	Samsum	Mean
Input OOD						
Dot product	AUROC ↑	97.76\pm0.11	98.75\pm0.07	99.87\pm0.06	99.46\pm0.09	98.96
	FPR95 ↓	11.07\pm0.74	4.75\pm0.41	0.00\pm0.00	0.02\pm0.02	3.96
Euclidean	AUROC ↑	74.22 \pm 0.65	84.43 \pm 0.23	97.06 \pm 0.41	98.30 \pm 0.23	88.50
	FPR95 ↓	90.20 \pm 0.37	74.08 \pm 1.04	15.27 \pm 5.30	7.17 \pm 1.94	46.68
Output OOD						
Dot product	AUROC ↑	93.37\pm0.54	92.62\pm0.65	98.04\pm0.29	98.30\pm0.11	95.58
	FPR95 ↓	23.12\pm1.98	29.93\pm2.89	6.36\pm1.60	6.83\pm0.64	16.56
Euclidean	AUROC ↑	87.67 \pm 0.74	88.17 \pm 1.80	96.50 \pm 0.57	91.28 \pm 1.79	90.90
	FPR95 ↓	65.62 \pm 3.90	66.04 \pm 4.38	22.34 \pm 5.36	53.89 \pm 7.80	51.97

Dot product and Euclidean distance. We compare using the dot product and the negative squared Euclidean distance for the attention pooling in AP-OOD. For a formal definition of attention pooling with the negative squared Euclidean distance, we refer to Appendix D.3. Table 9 shows that using the dot product works substantially better. This result aligns with the well-established observation that measuring similarity using the dot product in high-dimensional spaces is more effective than using Euclidean distance.